A CONTROL SYSTEM FOR AN ACTIVE WEARABLE LIFT ASSIST DEVICE

by

James Nolin

A thesis submitted to the faculty of
The University of Utah
in partial fulfillment of the requirements for the degree of

Master of Science

Department of Mechanical Engineering

The University of Utah

May 2012

The University of Utah Graduate School

STATEMENT OF THESIS APPROVAL

The thesis of **James Nolin**

has been approved by the following supervisory committee members:

Andrew S. Merryweather	, Chair	**1/4/2012** Date Approved
Donald S. Bloswick	, Member	**1/4/2012** Date Approved
Stacy M. Bamberg	, Member	**1/4/2012** Date Approved

and by **Timothy A. Ameel** , Chair of

the Department of **Mechanical Engineering**

and by Charles A. Wight, Dean of The Graduate School.

ABSTRACT

The goal of this project was to study a control system and prototype for a wearable lift assist device. The purpose of this device is to support the upper body during torso flexion and extension to reduce the erector spinae muscle activity and decrease back compressive force. It could also be used in rehabilitation or return to work scenarios after back injury or surgery. The proposed device is actively controlled and able to provide support based on the wearer's position, anthropometry, and desired level of assist. The upper body is supported by direct current (DC) motors and bilateral torsion springs. The assist level is a function of the percentage of torque needed to statically support the torso for a given angle and can range from 0 to 100%. To develop and test the control system, an electromechanical system was developed to simulate the human torso during lifting. The torso and support mechanism were driven by separate DC motors and drive trains. The torso and support of the mechanism were operated independently, as would be required of an actual assist device. The support control used a position sensor to approximate torso angle and a load cell to determine if the correct amount of torque was applied. The load cell also served to measure the amount of actual assistance provided and gave feedback to the control system.

The support control system and mechanism were evaluated using three angular trajectories, derived from actual lifting data. The measured trajectory of the torso with no assist was compared at each level (20 - 100%, in increments of 10%). Ten percent was

not analyzed because the support system was unstable at such a low assist level. The torso's trajectory, load cell measurements, and torque produced by the motor driving the torso were analyzed to determine performance. There was a statistical difference when comparing the torso's trajectory with no assist to each level of assist ($t < 0.0001$) but may not be practically different. No statistical difference was found when comparing the load cell measurement to the target value for each trial ($t > 0.05$). The torque produced by the torso motor was reduced for all trials and were statistically different ($t < 0.0001$).

This study demonstrates that a mechanism can be actively controlled to provide assistance during lifting. A feasible control system was developed and tested. System stability and mechanical losses in the apparatus were the primary sources of error. Further work on active lifting assist devices and studies to determine actual benefits to users is warranted. The next step is to develop a wearable prototype and explore the benefits of using it in rehabilitation, and low back pain relief.

TABLE OF CONTENTS

LIST OF FIGURES

Figure

LIST OF TABLES

Table

AKNOWLEDGEMENTS

I would like to express my sincerest gratitude to my advisor Dr. Andrew Merryweather, whose tireless efforts made this project possible. I am also grateful for the support of Dr. Donald Bloswick and Dr. Stacy Bamberg.

I want to recognize the encouragement and assistance of Christopher Brammer, as well as others in the Ergonomics and Safety lab.

Lastly, I want to thank wife, Lelauna, and my son Collin for their love and support.

1. INTRODUCTION

1.1 Background

Every day countless objects are being moved without any mechanical assistance (i.e., hoist, lift, etc.). Sometimes assistive devices are available but are not always used. Often this lifting is done frequently, involving high forces and awkward postures. These and other factors such as repetitive work, frequent torso flexion, and vibration are known to increase the risk of low back disorders (Kumar, 2008). There are also factors outside of the work place that can contribute to back pain and injuries. Problems with the low back are the most common musculoskeletal disorder and the most costly (Kumar, 2008). Back pain is the most common complaint heard by primary care physicians, after the common cold (Katz, 2006). Nonspecific back pain is a complaint of most patients who seek assistance from health care providers (LeBlanc & LeBlanc, 2010).

1.1.1 The Back

The following section briefly provides an overview of the back, in order to better understand how the proposed device would assist the back in lifting. The vertebrae in the back are separated into five distinct groups because of their shapes, cervical, thoracic, lumbar, sacral (or sacrum), and coccyx (see Figure 1.1). For the purpose of this study focus will be given to the lumbar region of the low back.

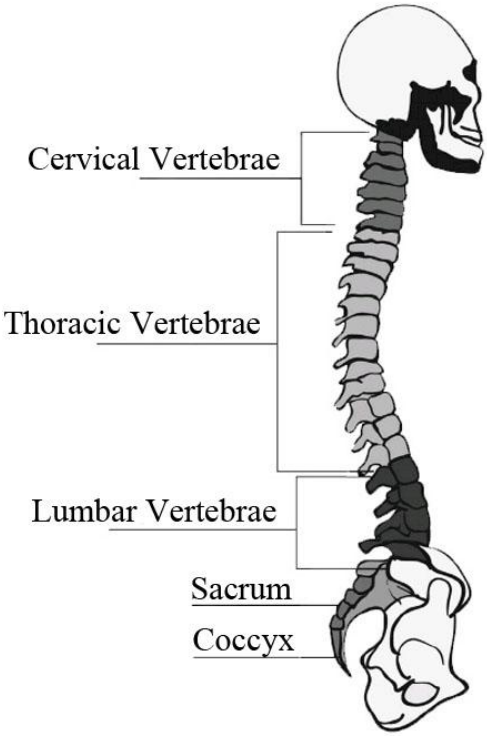

Figure 1.1: Regions of Spine (adapted from Marras, 2008)

The low back consists of ten vertebrae and three to five fused segments. Half of the vertebrae are lumbar vertebrae and are labeled L1-L5, shown in Figure 1.2. The other five vertebrae make up the sacrum and are labeled S1-S5 (Jenkins, 1991). These vertebrae are not individually labeled like the lumbar vertebrae and included for reference. The region where these vertebrae are located can be found in Figure 1.1 above. Between each vertebra is a vertebral disk, which connects the vertebrae together and absorbs shocks (Jenkins, 1991). The disks also allow adjacent vertebrae to move a small amount. Parallel to the vertebral column is a group of muscles called the erector spinae muscle group (commonly referred to erector spinae muscles). This muscle group is responsible for extending the spine and has multiple origin and insertion points at various vertebrae and ribs (Jenkins, 1991).

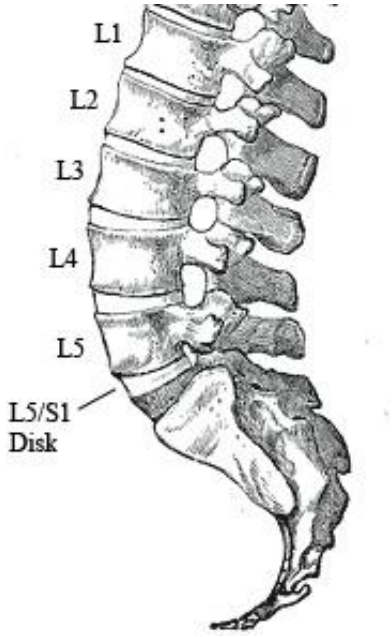

Figure 1.2: Lumbar Vertebrae (adapted from Gray, 1918)

1.1.2 Lifting

When the torso is flexed, gravity acts on the upper body. Gravity applies a torque or moment about the low back. Torque is force multiplied by the distance between the point of rotation and the location of the force. To counter this, the erector spinae muscles must generate an equal and opposite moment about the same point, in order to maintain balance. The muscles must produce a large force to generate an equal moment because of their close proximity to the disk between the L5 and S1 vertebrae (L5/S1). Figure 1.3 illustrates this using a simple free body diagram. This force compresses the disks in the back (back compressive force or BCF), which correlates to the highest incidence of low back pain (Kumar, 2008). The location of the greatest moment occurs at the L5/S1 vertebral disk, which is also at the greatest risk to injury (Waters, Putz-Anderson, Garg, & Fine, 1993).

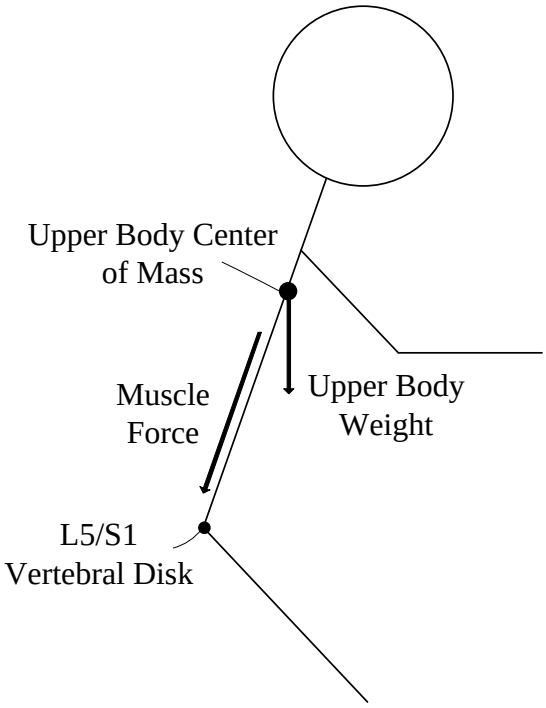

Figure 1.3: Simple Free Body Diagram with Torso Flexion

1.1.3 Scope of Problem

Low back pain/injuries are a significant problem in industry and cost businesses between $20-$50 billion a year (Pai & Sundaram, 2004). Often this requires time spent away from work and may require workers to be on light duty upon returning. In 2009, eight days was the median number of days spent away from work because of back pain/injury (BLS, 2009). Figure 1.4 shows the distribution of days spent away from work. Two thirds of low back pain costs, exceeding $100 billion in 1991, were indirect costs caused by reduced productivity and lost wages (Katz, 2006). Individuals ranging in age from 25 to 54 accounted for 78.5% of workers experiencing this type of injury, in 2001 (National Institute for Occupational Safety and Health, 2004). Of all the workers compensation costs, low back musculoskeletal disorders account for almost 33% (Snodgrass, 2011). Sometimes back surgery is used to treat back pain or back injuries,

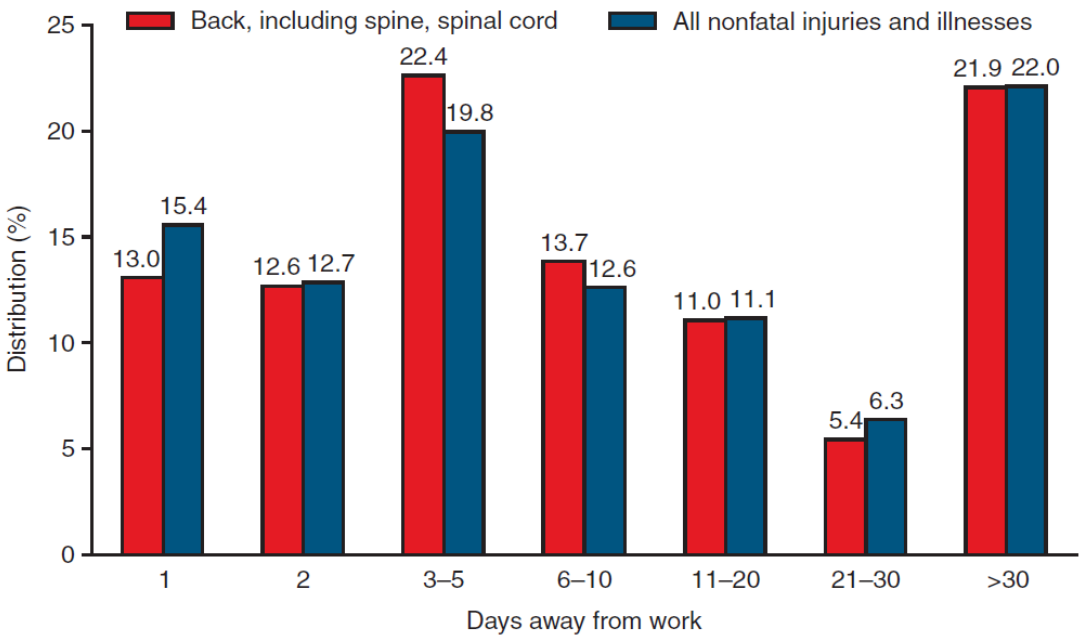

Figure 1.4: Distribution of Days Spent Away From Work (National Institute for Occupational Safety and Health, 2004)

requiring more time spent away from work. Spinal surgery has also increased in recent decades (Deyo, 2007). Figure 1.5 shows the incidence rate of back injures by industry. It is clear that all industries are affected. Back pain is also common in those with sedentary jobs, which implies there are other factors involved (Pope, 1989). There is strong evidence that returning to work after surgery is beneficial to those injured (McGregor, Burton, Sell, & Waddell, 2007). The United States Bureau of Labor Statistics reports injury rates for full-time employees on four areas of the back thoracic, lumbar, sacral, and coccygeal. Table 1.1 shows the incidence rate of injury and illness of the vertebral regions. The lumbar region had the highest injury rate by far, at 11.3 per 10,000 workers (Bureau of Labor Statistics, 2009). This was more than 11 times region with the next greatest injury rate. As a result, the goal of a back rehabilitative device should be to reduce the stress in this area.

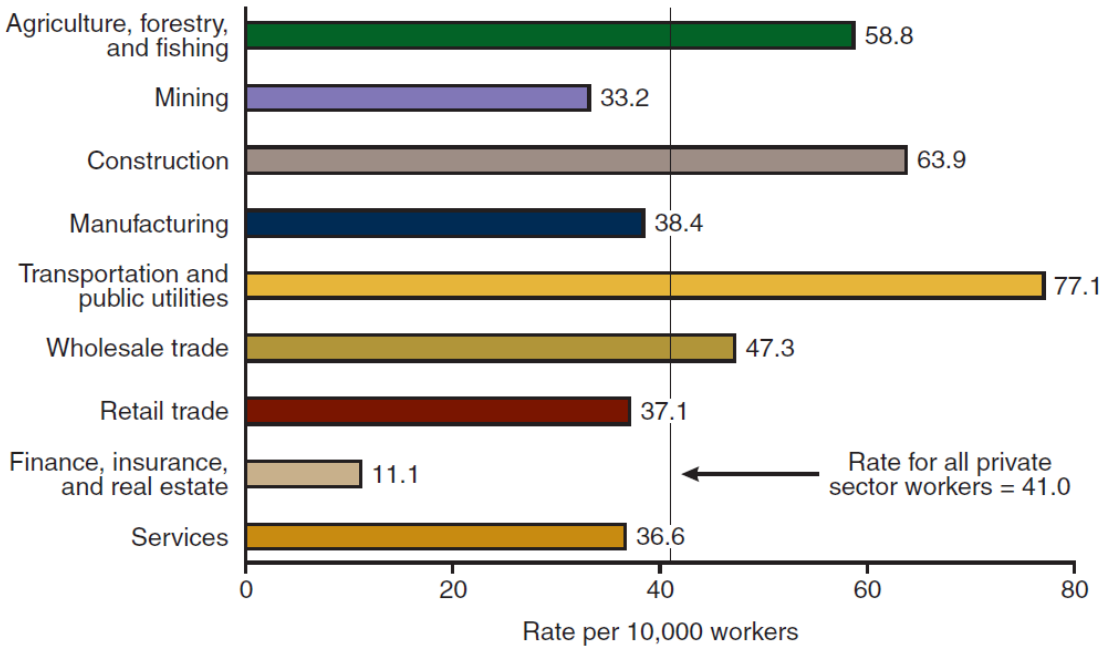

Figure 1.5: Incidence Rates of Back Injuries by Industry (National Institute for Occupational Safety and Health, 2004)

Table 1.1: Injury and Illness Incidence Rate by Vertebral Regions (Bureau of Labor Statistics, 2009)

Region	Incidence Rate per 10,000 Workers
Thoracic	1.0
Lumbar	11.3
Sacral	0.0
Coccygeal	0.2

Currently no devices are known to exist which actively support the torso during flexion that determines force based on vertical torso angle. The University of Berkley and other organizations have created exoskeletons and similar devices for the purpose of enhancing human performance. It is likely none of these devices however, could serve as a rehabilitation device, or support/assist the torso in the occupational setting. The closest device that could be found is a personal lift assist device (PLAD) developed at Queen's

University in Ontario, Canada. This device is passive and uses elastic bands attached to the calves, which stretch as the torso flexes, to generate torque. As a passive device, it has a limited range of assistance and is also linear. The torque required is not linear, however. It varies by the sine of the torso angle when the angle is measured from vertical. Therefore, the best results would likely be from an electric motor or other actuator.

1.1.4 Purpose of Research

The purpose of this research is to develop a control for a lift assist device to be worn by someone who experiences back pain or recently had back surgery. The device would be used to support the upper body. It would be limited to assist along a single axis of rotation, neglect asymmetry and neglect load in the hands. The control would have three user supplied parameters, height and weight of the user, and the desired assist (given as a percentage). The control would enable the device to follow the wearer's movements without interference and provide the desired assist throughout normal torso movement. The control system would not be used to increase or enhance human performance, but to reduce the force the muscles must generate during lifting. Over time the amount of assist can be reduced, requiring more force be generated by the muscles. The device would be able to support a variety of anthropometries ranging from a 5^{th} percentile female to a 95^{th} percentile male. Sensory inputs include angle of the upper body portion, from vertical and angle of the lower body portion relative to the upper body portion. Inputs would also include force sensors placed at the shoulders. The angular measurements from the device would be used to estimate the body's position.

Based on the previously described inputs, the correct amount of torque would be generated for torso motion with no asymmetry, when the torso was between 0 and 110 degrees from vertical. The magnitude of the muscle and support forces would vary depending on level of assist and torso position. As previously mentioned, the amount of load the back has to support contributes to back injury/pain. Since upper body weight is a part of this load, partial support should reduce the stress on the low back and reduce erector spinae muscle activity. By supporting the torso, those recovering from back surgery and low back pain may be able to return to work more quickly and may be allowed to lift more if on light duty. The support would be provided by applying a force close to the shoulder. Figure 1.6 shows a free body diagram illustrating the approximate location of support. Applying such a force should reduce muscle activity in the low back. Some muscle force will still be needed even when the device is fully supporting the torso the device would respond to torso movement.

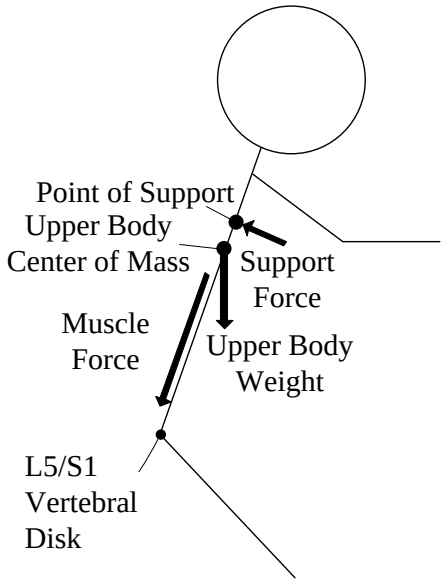

Figure 1.6: Support Free Body Diagram

2. METHODS

In this chapter the methods of developing the control and constructing the test apparatus are discussed. Also addressed are assumptions made, the procedures for testing the control system, and data collection procedures.

2.1 Test Apparatus

Since the goal of this project was to develop a control for a wearable lift assist device a test apparatus to simulate was constructed. A support system was needed also to test it. The following sections describe both systems. The next two sections provide details about each structure as well as anything unique to that system. The drive and electrical systems are addressed in later sections and are not separated by system because of similarities. A figure of the test apparatus can be found in Figure 2.1.

The apparatus has three major parts, the torso, the support, and the drive trains. The drive trains were essentially the same. The largest difference was the size of one sprocket. Measures were taken throughout the design and construction phases to reduce the complexity, time, and cost to build the apparatus. First, because of symmetry the torso was only supported on one side. Also, the design incorporated as many parts which were already available as possible. However, some parts still needed to be modified and a few custom parts were necessary.

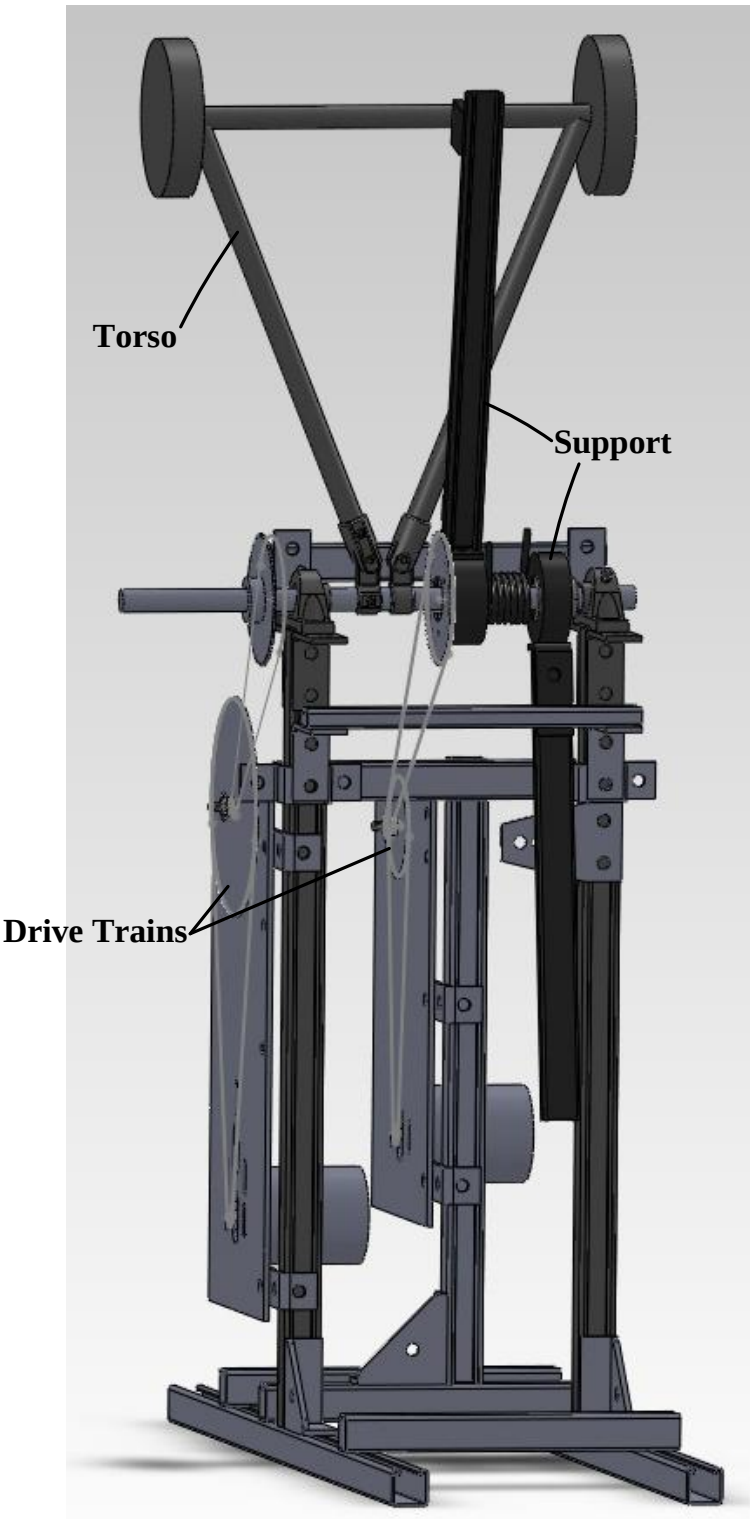

Figure 2.1: Test Apparatus

2.1.1 Torso Structure

The torso structure consists of four components (see Figure 2.2):

1. Base
2. Legs
3. Waist
4. Torso

The three latter are so named because of their function relative to the human body. The base of the system consists of four pieces of strut channel laid out to form a rectangle. The length of the base is much greater than the width, to add stability during operation.

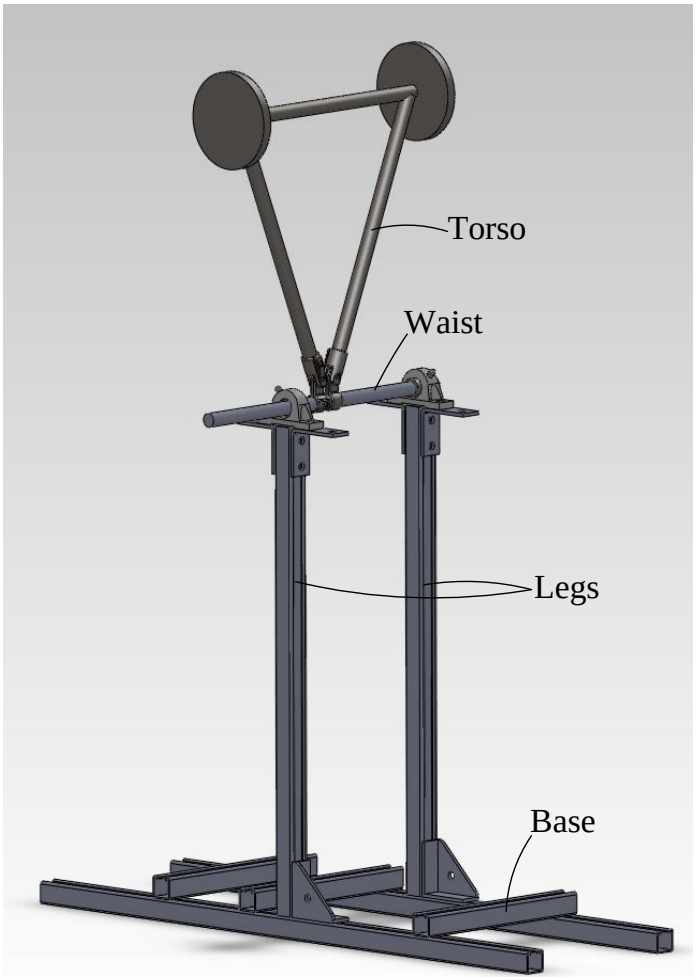

Figure 2.2: Torso Structure

Two additional pieces of strut channel were used to form the “legs” of the apparatus and mounted to the base. The open part of the channel faced forward to facilitate proper chain tension, which is addressed in a later section. Mounted bearings were attached to the leg members using four right angle brackets, two for each side. A steel shaft was placed in the bearings to create the waist. The torso was made by welding three steel tubes together, forming an inverted triangular shape, shown in Figure 2.3.

The torso was rigidly connected to the waist shaft using slip-on rail fittings with set-screws. The rotation of this shaft, and consequently, rotation of the torso were used to simulate torso movement during lifting.

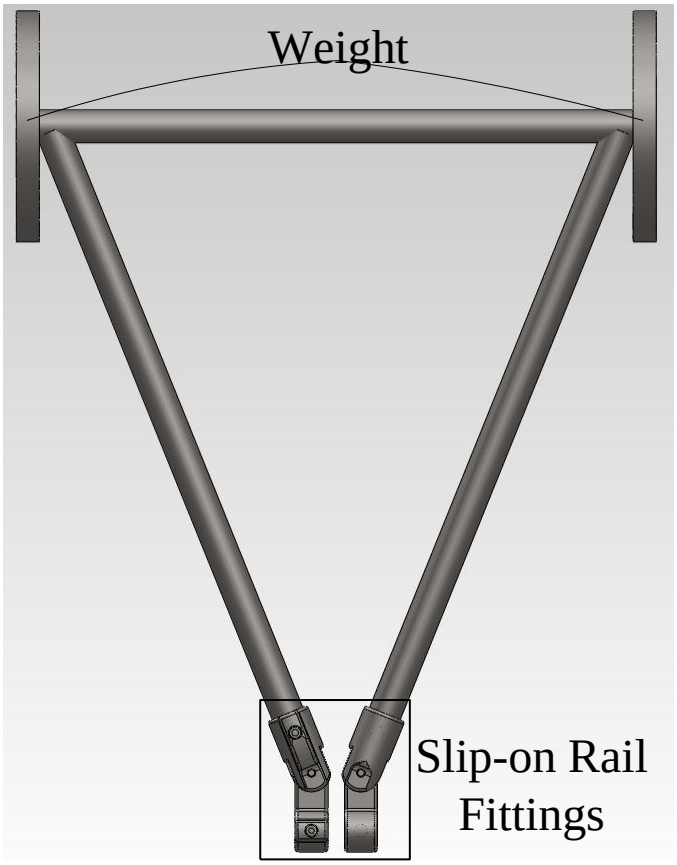

Figure 2.3: Torso

The height and width of the waist and torso, as well as the leg lengths, are all calculated using body segment parameters by Drillis and Contini, 1966. Weight was added to the torso to simulate body weight. For simplicity it was placed at the top of the torso, as opposed to the approximate location of the center of mass in a human torso. The weight was mounted by placing a threaded shaft through the tube and adding weight, in equal amounts, on each side.

2.1.2 Support Structure

The purpose of the support structure is to provide a means of testing the control system. It needed to function similarly to a potential device that could be worn and assist the torso structure in the same way. To that end, the support contacts the torso and legs of the torso structure. The part of this structure which contacts the torso, at the shoulder, is referred to as the torso support. The part which contacts the leg is referred to as the leg support. Both supports consisted of a custom cylindrical piece which rotates freely about the waist shaft. The strut channel was attached in a radial direction to each cylindrical piece and contacted the torso and a bracket attached to the leg. A torsion spring was placed between them, concentric with the waist shaft. Figure 2.4 shows the support structure with the aforementioned parts labeled.

The spring is energized as the torso and torso support rotate, providing additional support. The purpose of the spring is to supplement the required motor torque, allowing a smaller and less expensive motor to be used. It added stability by causing the support to maintain constant contact with the torso. The support motor and accompanying gear train was designed to support 100% of the upper body at 90 degrees of torso flexion.

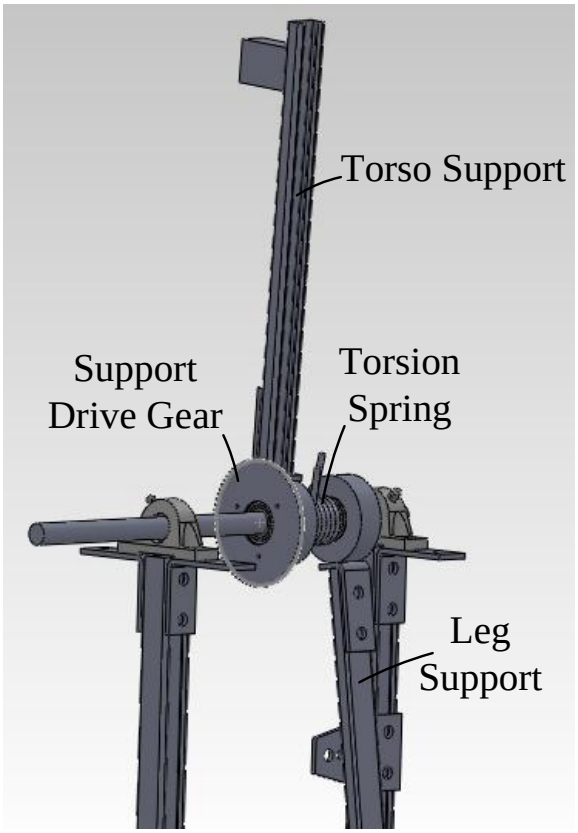

Figure 2.4: Support Structure

The purpose was to simulate how the device would behave when used on a moving body and test its viability. Force sensors were placed where the supporting members contact the upper body, at the shoulder, and upper leg to measure forces. These data needed to be collected to determine if the device is supporting the torso as expected. Also, these data could be useful in determining the feasibility of redirecting the forces on the body, to generate a torque to support the upper body.

2.1.3 Drive System

Both systems used direct current (dc) motors to generate torque. DC motors were used instead of alternating current (ac) motors because of their simplicity in control.

Both dc motors were controlled using Advanced Motion Controls Analog Servo Drive, model 30A8T. The maximum possible torque each motor could generate with a simple gear train was insufficient, so a two-stage compound gear train was used for each. The compound gear consists of a custom sprocket welded to a commercially made sprocket. The custom sprockets were necessary because one could not be found with the correct number of teeth for the desired ratio. Each motor was mounted to a custom steel plate along with the compound gear. Slots and holes were cut out of the plate accordingly. Slots were used so the motors could be shifted vertically to adjust chain tension. A shoulder bolt served as the shaft for the compound gear. The plates were attached to vertical frame members. For the case of the torso motor, its mounting plate was attached to a leg member. The gear train and dc motor driving the torso are referred to as the torso gear train and torso motor, respectively. Also, the gear train and dc motor driving the support are called the support gear train and support motor, respectively. The output sprocket of the torso gear train was attached to the waist shaft, while the output gear of the support gear train is attached to the support drive gear (shown in Figure 2.4). Figure 2.5 shows the torso drive system. The support drive system is similar, except it has different sprocket sizes and the output gear is the support drive gear.

The torso motor could be analogous to two muscle groups, the erector spinae muscles and rectus abdominus. Positive torque (torso extension) produced by the torso motor is analogous to the moment the erector spinae muscle generates about the L5/S1. Negative torque generated by the torso motor is analogous to the rectus abdominus muscles producing a force during torso flexion.

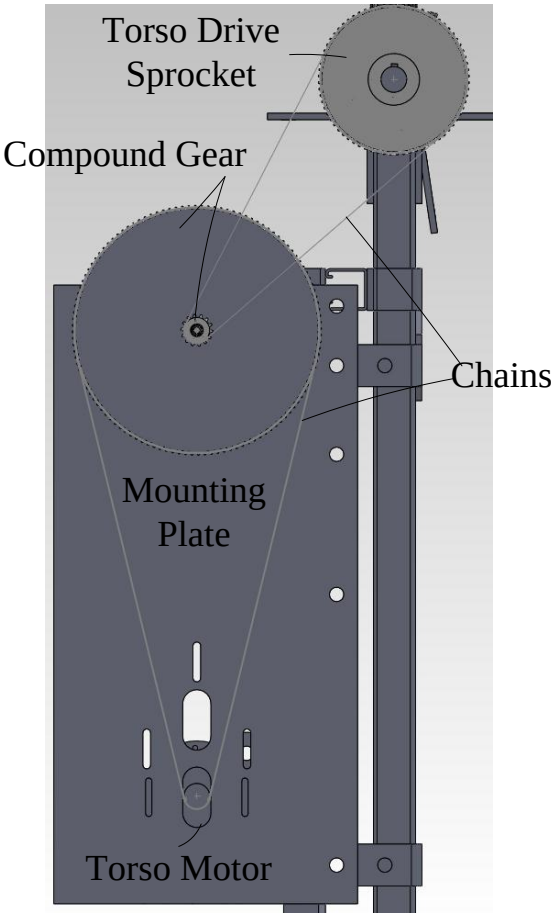

Figure 2.5: Torso Drive System

2.2 Design Criteria

The specifications for the dc motors and drive trains were determined by calculating how much torque would be required to statically support an average male's upper body at 90 degrees from vertical. Because the proposed device would have two motors, each supporting the torso, this torque was divided in half. In the end, the most economically feasible motor was used, which became the center for the design. Originally the goal was to use the weight of a 50^{th} percentile male but it was not practical to design an apparatus that could handle that much load. The weight added to the torso was reduced until the desired performance was achieved.

2.1 Sensors

The apparatus uses two types of sensors, position and load. The following sections describe both types, their function, and use. The locations of each sensor's attachment point are illustrated in Figure 2.6.

2.1.1 Position Sensors

To measure the angle of the upper body and torso support, two position sensors were used. The position sensors were made by Space Age Control, Inc. (part number 160-1285-C8SS). An image of one of the sensors can be found in Figure 2.7. Each sensor has a wire that is attached to the objected being measured. As the wire changes length, a potentiometer turns producing a change in voltage. This change in voltage has a linear relationship with the change in wire length, allowing distance to be measured. The wire of each sensor was rigidly attached to the waist shaft and support. As each rotates,

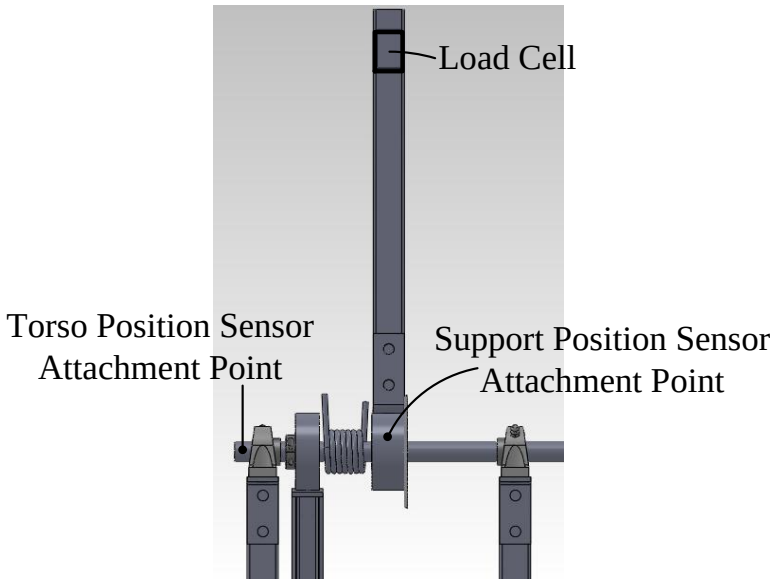

Figure 2.6: Sensor Attachment Locations

Figure 2.7: Position Sensor

the wire extends or retracts, depending on the direction, providing a measure of angle. Since the data acquisition card used only had two outputs capable of supplying 10V, the position sensors were powered using a driver. The position sensors were supplied with 10V instead of 5V because the torso position sensor did not experience a large enough voltage difference to provide adequate resolution.

2.1.2 Load Cell

Force was measured using a commercial load cell made by Interface, model SM-500. Figure 2.8 shows the load cell used. Although the load cell is able to read both compressive and tensile forces, only compressive force was necessary to use. This is

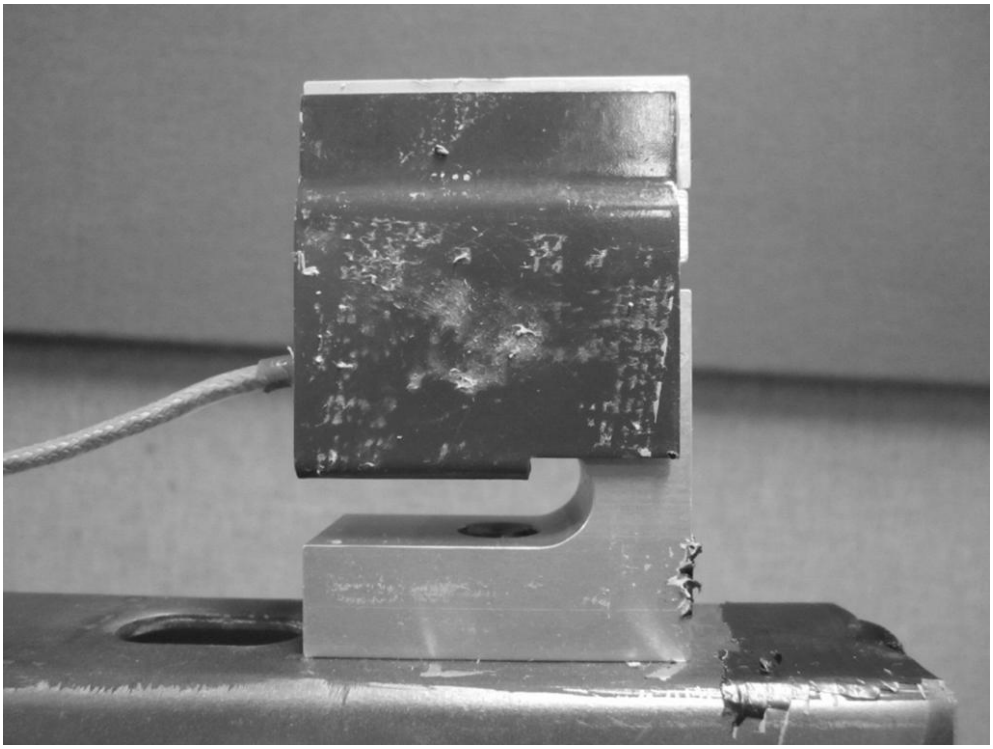

Figure 2.8: Load Cell

because the system is responsive enough to always measure a force. If this were not the case, tensile force would be necessary to provide feedback and follow torso movement properly. Silicone was attached to the top surface of the load cell to protect the load cell.

2.2 Electrical System

Each motor has its own driver and power source. The power source consisted of two 12 V lead acid batteries, connected in series to supply a total of 24 V. To control the flow of electricity to the driver, relays were used in place of mechanical switches because of their ability to handle higher currents. A mechanical switch was used in each circuit to activate the relay. Figure 2.9 shows the wiring diagram for the electrical system. The electrical systems for both motors were identical.

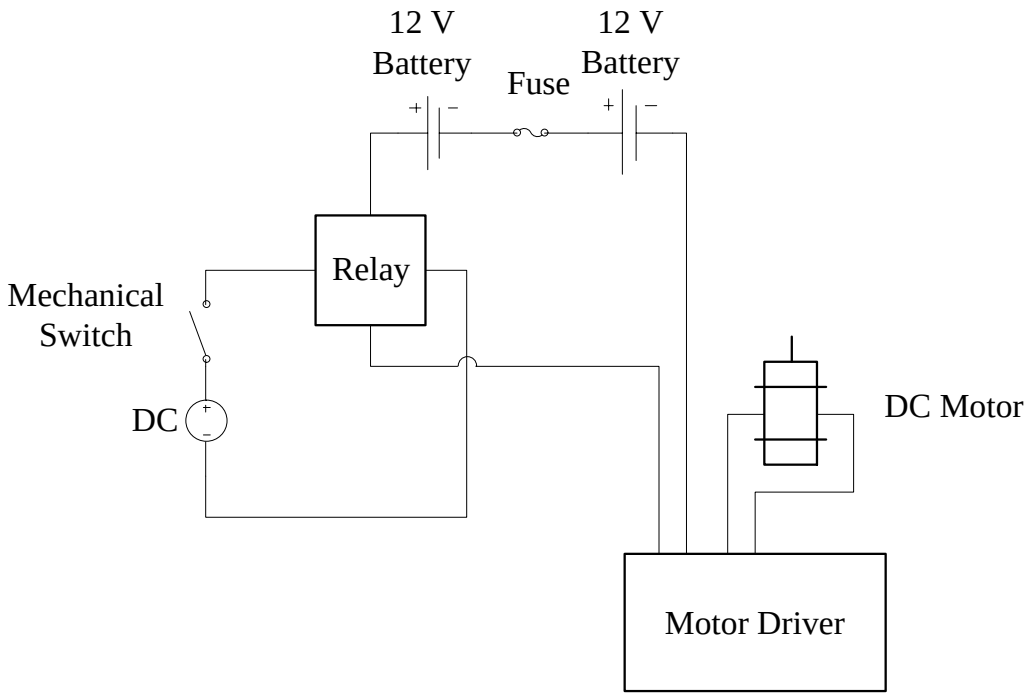

Figure 2.9: Motor Electrical System Wiring Diagram

2.3 Safety

In designing and using the apparatus, safety was a primary concern. Both potential physical and electrical hazards were considered. For example, fuses were placed in each circuit to prevent overload. Also, multiple software and physical switches can be used to activate or deactivate each motor independently or simultaneously. Because the relays require a separate dc power source, which is dependent on a wall outlet, the system will turn off if a power failure occurs in the building. Torso rotation was limited by both software and physical restraints. If the torso moved outside of a specified range, the software instructed the motor driver not to supply any voltage to the torso motor. If it continues to rotate, hard stops (see Figure 2.10) were placed to limit movement.

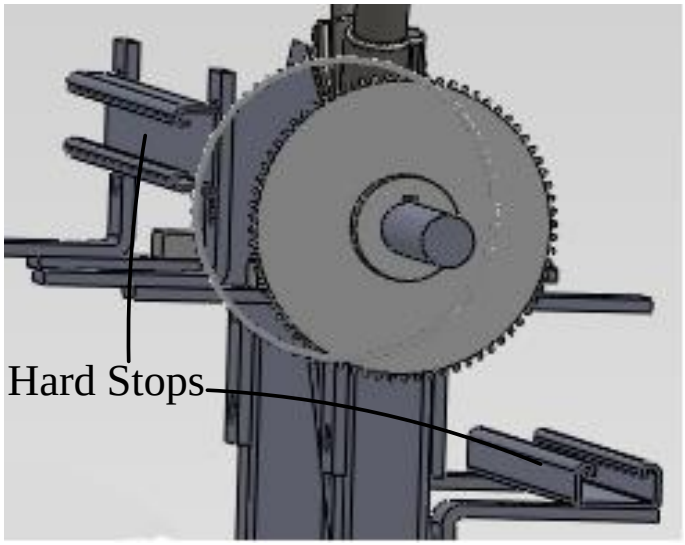

Figure 2.10: Hard Stop Locations

2.4 PID Control

Since a proportional control is used to control the torso and a proportional, integral, and derivative (PID) control is used to control the support, a brief overview will be provided. A PID controller has two inputs, the set point and the process variable. The set point is the desired output or target value. The process variable is feedback from a sensor and is what needs to be controlled. A PID control focuses on reducing the amount of error between the set point and process variable. It consists of three elements (named previously), which are summed together to get the output response. Each element has its own gain which changes its contribution to the output. These changes are defined in Figure 2.11. The proportional gain affects rise time or how quickly the process variable gets close to the set point. Increasing the proportional gain will usually increase the amount of overshoot. The integral gain sums up the error over time, reducing steady state error. Finally, the derivative gain will increase system response and will decrease overshoot. However, it is sensitive to noise in the process variable.

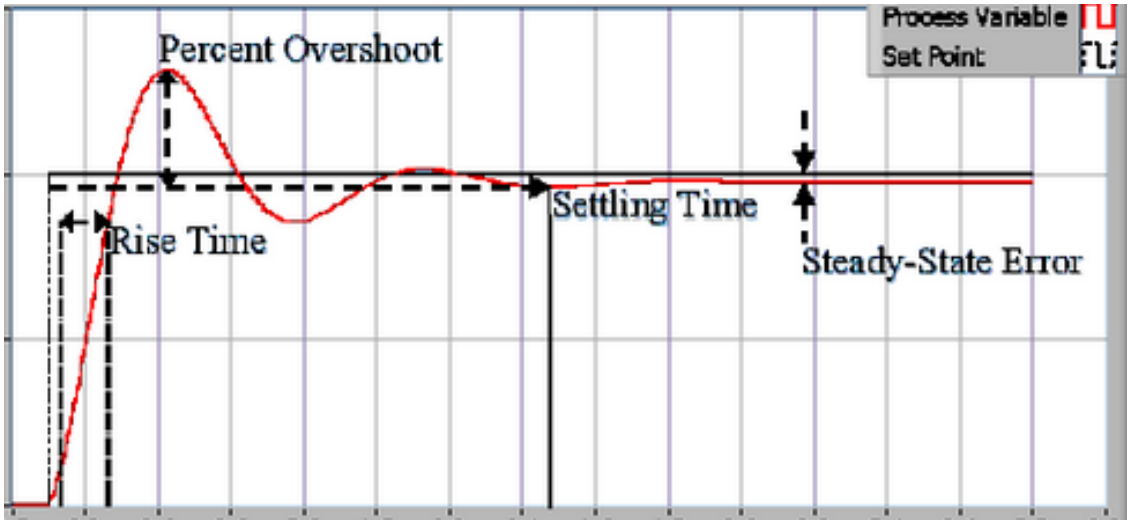

Figure 2.11: PID Control Response (adapted from National Instruments)

2.5 Control

The control systems were developed using LabView, made by National Instruments. LabView was used because the ease of working with a graphic interface and the ability to see data in real-time. The system required two independent control systems, one to control the torso and the other to control the support. Both control systems were created in the same Virtual Instrument (VI) because of convenience and the potential difficulty in having two VIs trying to access the data acquisition (DAQ) card at the same time. It was paramount that the support operates without having any information about future positions or current torso angle. The DAQ card used for control and data collection was a PCI-6052E, made by National Instruments. Attached to the DAQ card was a BNC terminal block (model BNC-2090) also made by National Instruments. Because two motors were used in the system, a control system had to be developed for each. To provide a better understanding of the overall system, Figure 2.12 shows the wiring diagram of the entire electrical/sensor system.

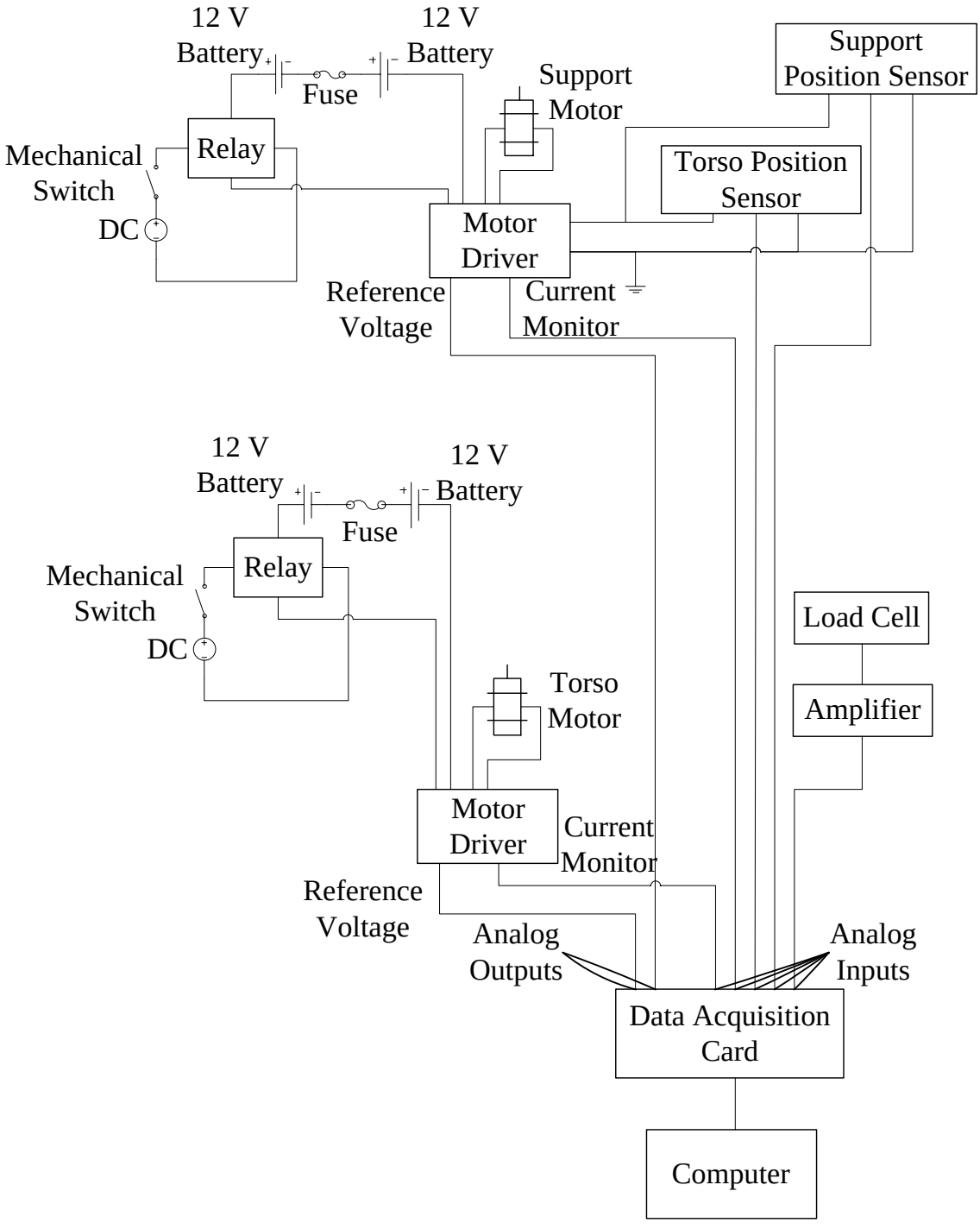

Figure 2.12: System Wiring Diagram

2.5.1 Torso Control

The torso was controlled by using a position control method. A block diagram showing the logic used to control the torso can be found in Figure 2.13. A proportional controller was used to control the torso. The integral and derivative gains were set to zero because they introduced undesired behavior. The integral gain introduced additional overshoot and the derivative gain introduced jitter caused by noise in the position sensor. The set point was determined by converting the current target angle to a voltage. The process variable for the controller is the voltage measurement of the torso position sensor. The control tried to equalize these two values, by moving the torso until the process variable closely matches the set point. To adjust performance, the proportional gain was varied until the desired response was achieved. Based on the gains and current position, the appropriate voltage is sent to the motor via the driver. This is repeated every time the loop is run. Everything within the dark-lined rectangle is in a while-loop, which repeats until the torso reaches within ±3 degrees of the last desired position or if a stop button on the front end is pushed. Before the start of an angular trajectory the control waited for 8 seconds. The delay was introduced because of the software Butterworth filter initially used to filter the position sensor signal. Because of the filter, a few seconds were needed for the system to measure the correct angle. The Butterworth filter was replaced with a median filter because of lag introduced into the system. The lag caused events to be missed such as if the torso or support exceeded a certain position threshold. The delay was left in the control so the trajectory could be aborted, if needed. It also allowed the support time to apply the desired amount of force to the torso, at the point of contact.

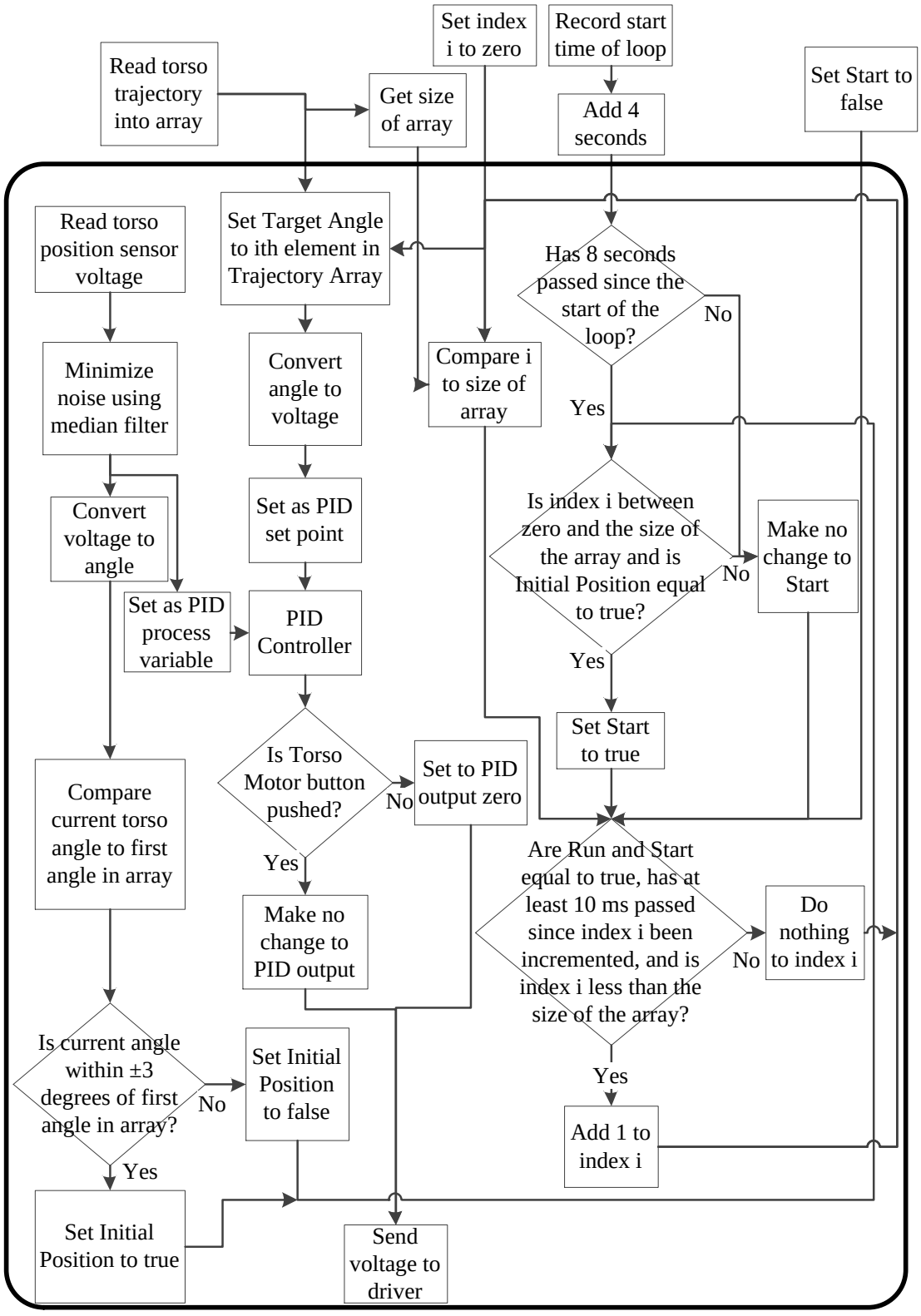

Figure 2.13: Torso Control

2.5.2 Support Control

For the support control, torque mode was used for the motor driver. Torque mode is such that current supplied to the motor is managed, instead of voltage. As a result, motor torque can be directly controlled. The equations used to calculate the voltage outputted to the driver to achieve the desired torque are as follows. Equation 2.1 shows the relationship between torque and current, in a dc motor, where τ is the torque generated, k_τ is the torque constant of the motor, and i is the current drawn.

$$\tau = k_\tau \, i \qquad \text{Equation 2.1}$$

Equation 2.2 shows the linear relationship between the input voltage and current, where i is the current being supplied to the motor, m is the slope of the calibration, V is the voltage sent to the driver, and b is the y-intercept of the calibration.

$$i = mV + b \qquad \text{Equation 2.2}$$

Equation 2.3 is derived by substituting Equation 2.2 for i. This equation is necessary to relate the driver input voltage to the motor current.

$$\tau = k_\tau(mV + b) \qquad \text{Equation 2.3}$$

Solving for V gives changes the independent variable from voltage to torque (see Equation 2.4).

$$V = \frac{\tau - k_\tau b}{k_\tau m} \qquad \text{Equation 2.4}$$

Using this equation, the voltage is calculated to achieve the desired torque from the motor. The following sections describe the evolution of the support control. While there have been several variations, the two largest are presented, along with the final version.

2.5.2.1 Design 1

The first design calculates the torque needed to support the torso at its current angle and according to the percent assist specified. The estimated torque the torsion spring is contributing is subtracted from this value. Equation 2.5 was the function used to make this calculation where P_a is the percent assist (as a decimal), F_{90} is the force needed to fully support the torso, at the shoulder, at 90 degrees, d_{LC} is the distance between the waist shaft center and the point of contact on the load cell, θ is the estimated torso angle from vertical, k_s is the spring constant of the torsion spring, and θ_s is the support angle also from vertical.

$$\tau_s = P_a F_{90} d_{LC} \sin\theta - k_s \theta_s \qquad \text{Equation 2.5}$$

In this design the role of the load cell was to determine the direction of the torso. Three cases were considered, torso extension, maintain position, and torso flexion. These cases were called Case 1, Case 2, and Case 3, respectively. To determine which case was occurring, a range of values was created centered on τ_s. Case 1 occurred when torque measured was less than the lower limit. Case 2 occurred when the measured torque was within the range. Case 3 occurred when the measured torque exceeded the upper limit.

Case 1 required more torque than provided by the result of Equation 2.5 so a second term was added giving Equation 2.6.

$$\tau = \tau_s + x_1\tau_s \qquad \text{Equation 2.6}$$

Since Case 2 indicated that the support was providing enough assist, no additional term was needed and the torque supplied by the system was simply τ_s. Case 3 was similar to Case 2 except the torque was reduced, shown in Equation 2.7.

$$\tau = \tau_s - x_2\tau_s \qquad \text{Equation 2.7}$$

The values of x_1 and x_2 were determined using trial and error, with 0.3 for each providing the best results. Figure 2.14 shows a comparison of the target torque and measured torque. As can been seen in the figure the torso is not well assisted during lifting, leading to Design 2.

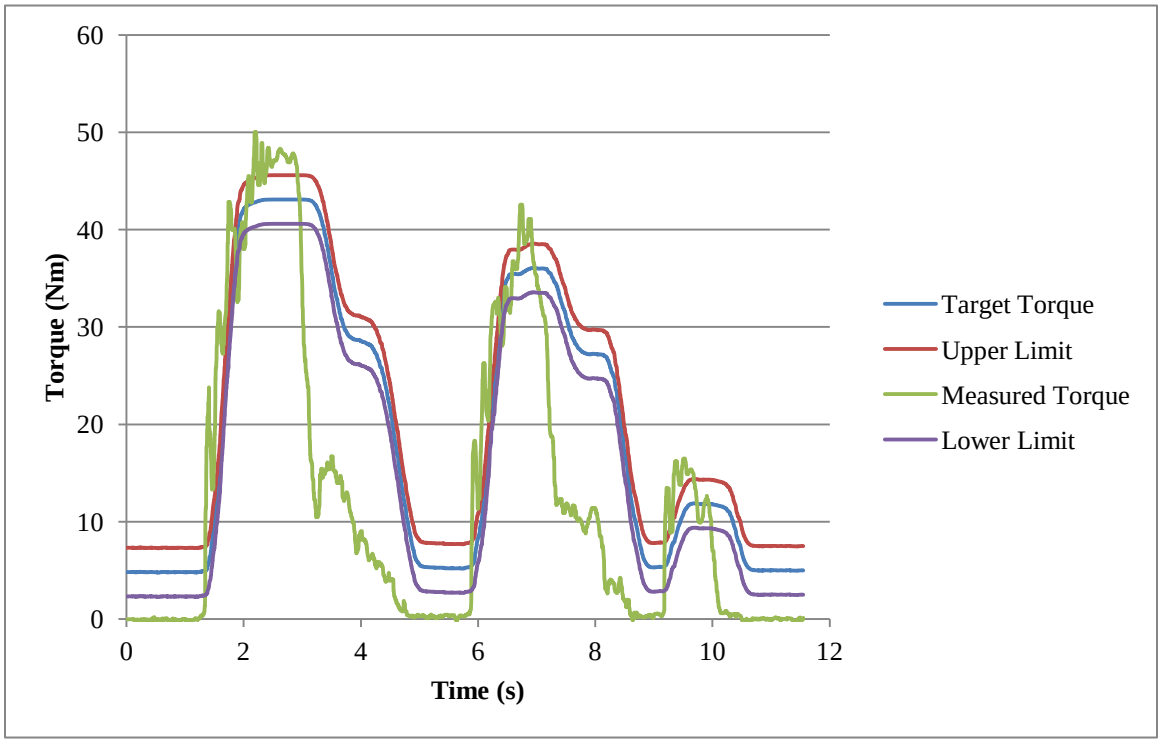

Figure 2.14: Design 1 Target and Measured Torque Comparison.

2.5.2.2 Design 2

The second design was similar to the first. A third term was added to Equation 2.6 and Equation 2.7 so the motor would provide adequate torque during lifting. This term starts at zero when one of the limits was crossed and increased in magnitude by a constant, each iteration of the loop. The amount of torque supplied by the support motor increases or decreases (depending on the case) until the measurement is within the acceptable range. The longer the torque measured is outside of the acceptable range, the larger it becomes. Once within the range the third term is set to zero. Different values for the constant were tested to get the best response. If the constant was too high, it would overshoot and switch between all three cases quickly. When the constant was too small the support would not respond quickly enough. The result of this change can be found in Figure 2.15. The torso was better supported during lifting; however the support was variable and provided too much support the torso was fully extended.

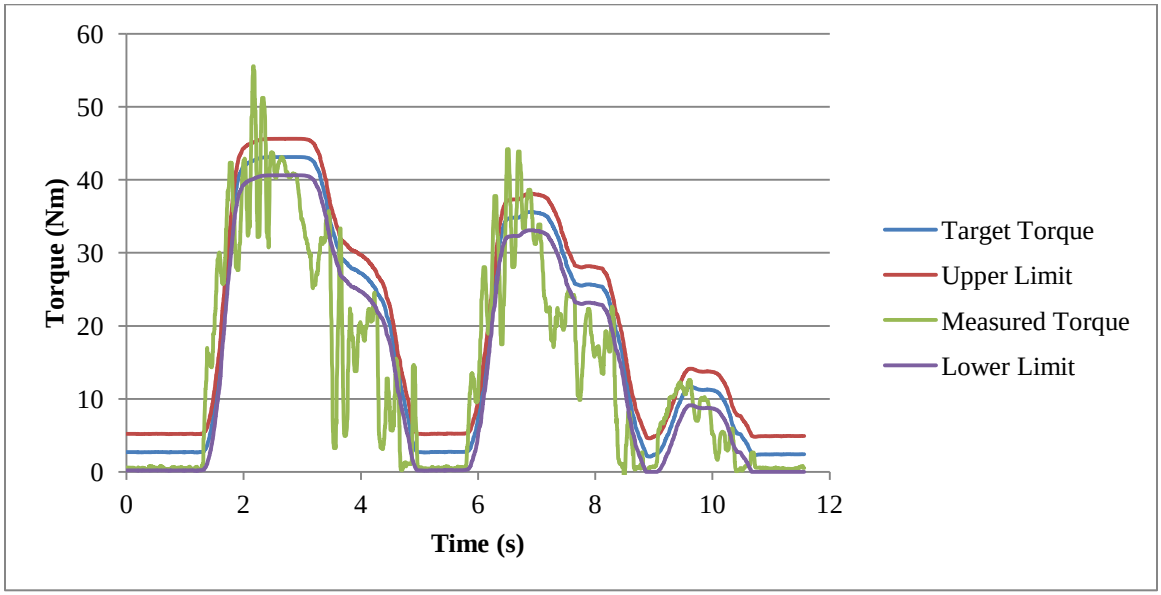

Figure 2.15: Design 2 Target and Measured Torque Comparison

2.5.2.3 Design 3

The third redesign took friction into account when calculating τ_s. An experimentally determined equation of friction, $F_f(\theta)$, was F_{90} became F shown in Equation 2.8 where is the equation for friction found experimentally. The procedure for determining this equation is described in Section 2.7.1.

$$\tau_s = P_a(F_{90} - F_f(\theta))d_{LC} \sin\theta - k_s\theta_s \qquad \text{Equation 2.8}$$

Designs 1 and 2 were revisited using the new equation for τ_s. Figure 2.16 and Figure 2.17 show the results of Designs 1 and 2 with and without friction ($F_f(\theta) = 0$). The support provided unstable assistance throughout torso flexion and did not adequately provide assistance during extension. As a result, a fourth and final redesign was necessary.

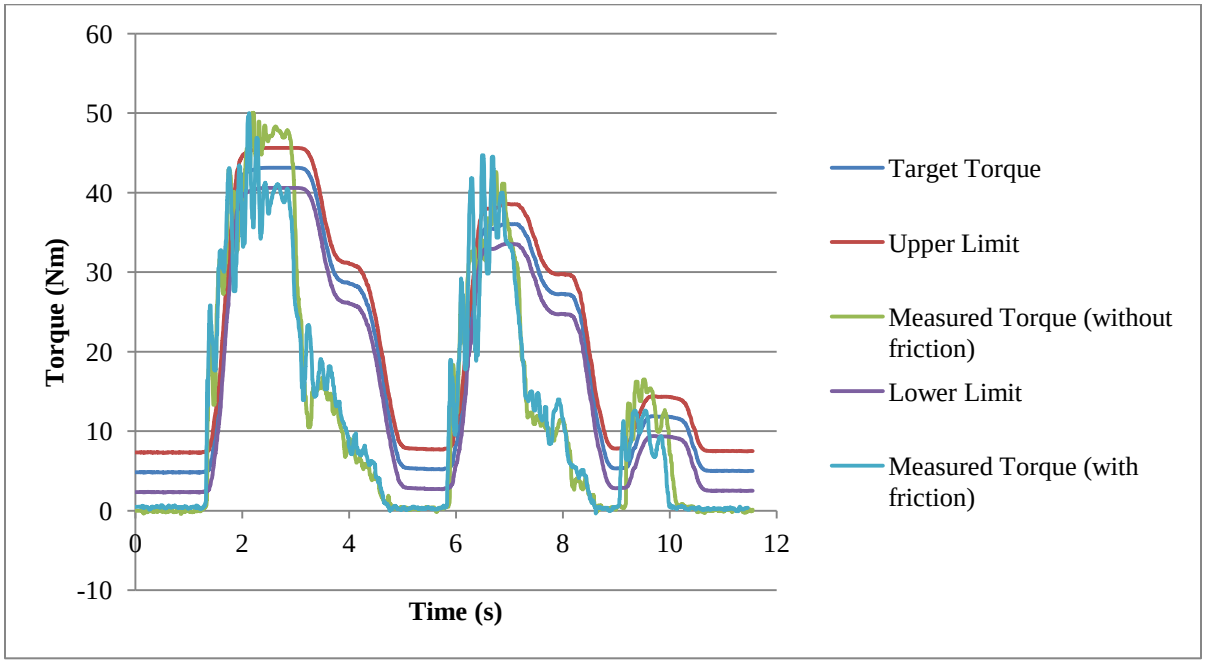

Figure 2.16: Design 1 Friction Comparison

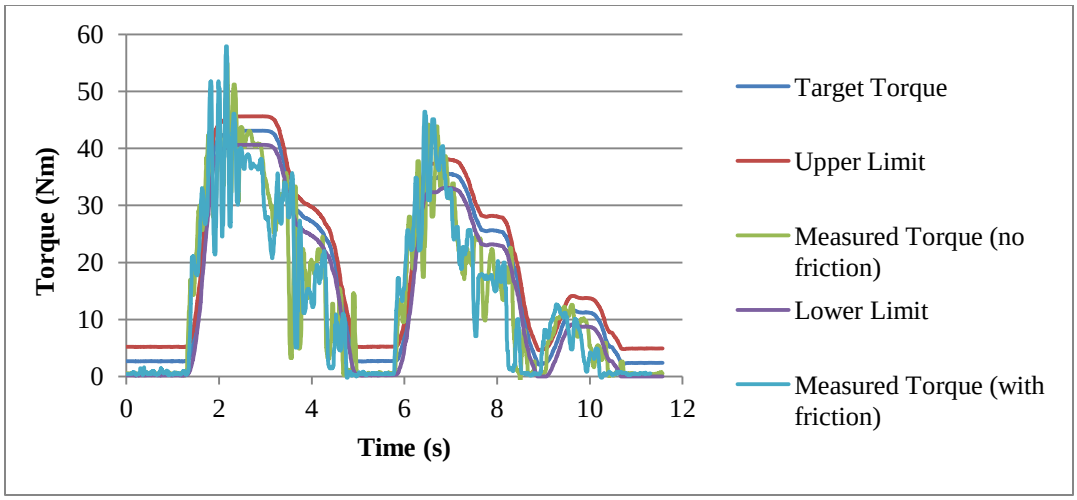

Figure 2.17: Design 2 Friction Comparison

2.5.2.4 Final Design

The final design differed from those previous because Equation 2.6 and Equation 2.7 were not used. These equations were replaced by a PID control. Also, the acceptable range of torque measurements was removed and consequently the three cases described earlier. They were replaced because the PID gave better response during lifting and provided more assist. Figure 2.18 shows the same trajectory for comparison. The figure indicated the torso is supported all the time.

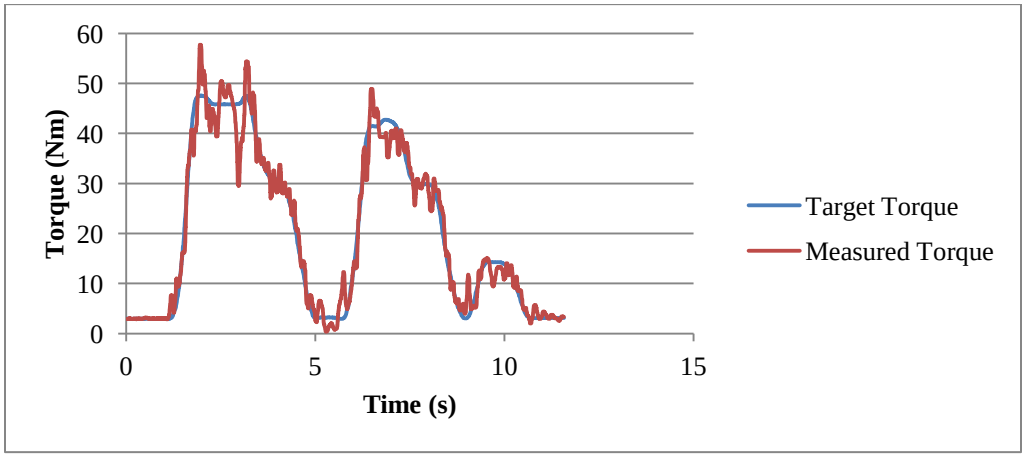

Figure 2.18: Final Design Assist and Measured Torque Comparison

The upper and lower limits were removed because the support performed better without them. Data with the limits in place were graphed and are found in Figure 2.19. The support did not follow the torso as well because when the measured torque is within the acceptable range, the system did not compensate for motion. This is visible in

Figure 2.19. During lifting the support recognizes it is not applying enough torque and as a result increases the amount of torque generated until the lower limit is exceeded. The system then does not respond to torso movement until the measured torque falls below the lower limit again.

Figure 2.20 shows a flow diagram illustrating the logic used to control the support. The support on/off button is a software button on the frontend of the VI. The load cell caused an approximate 12 degree separation between the support and the torso necessitating the correction.

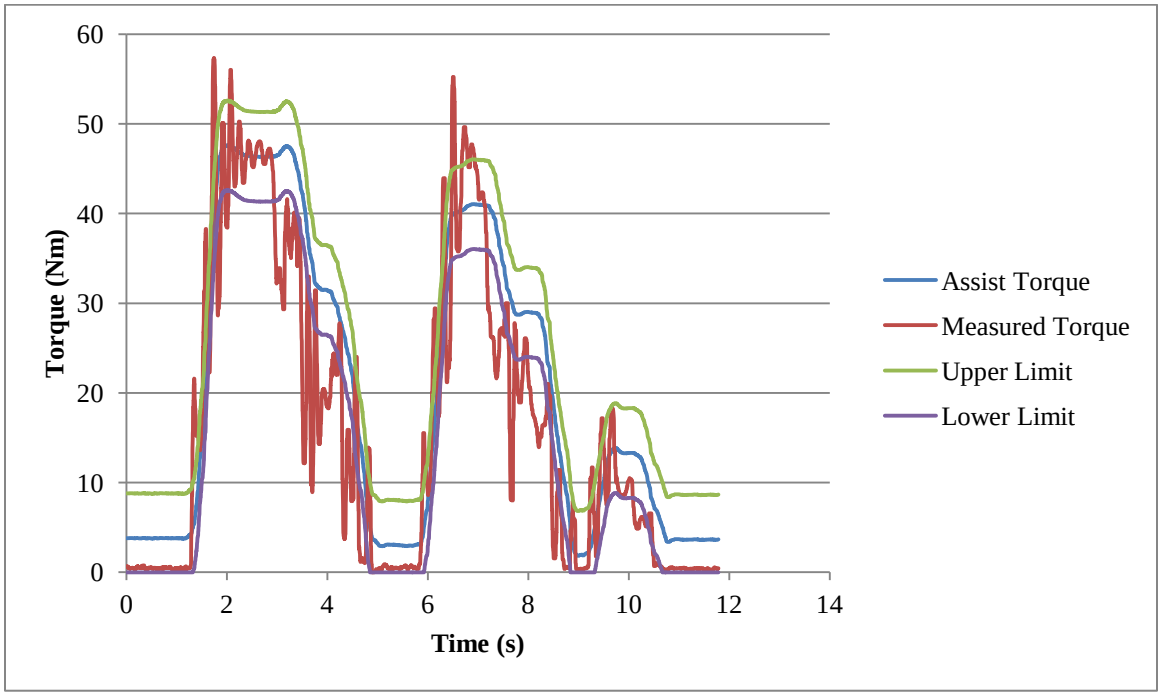

Figure 2.19: Final Design with Upper and Lower Limits

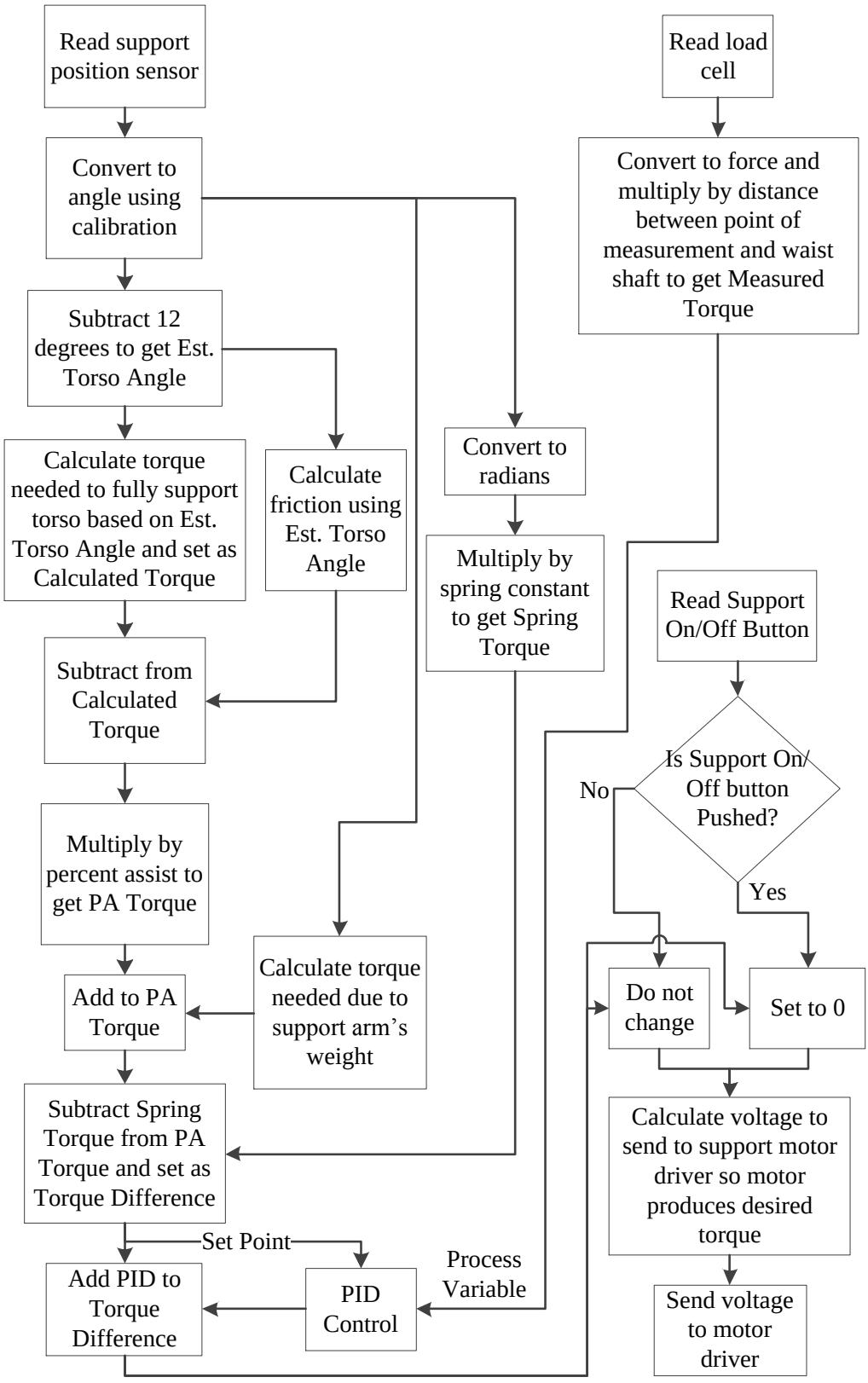

Figure 2.20: Support Control Flow Diagram

2.6 Calibration

To ensure accurate measurements, the position sensors and load cell had to be calibrated periodically. Each position sensor was calibrated by placing the torso and support at horizontal and vertical, recording the voltage at each point. The slope and y-intercept were calculated for a line intersecting each set of points. The load cell was calibrated by applying a known compressive force to the load cell and measuring the voltage output. Ten loads were applied between 0 and 100 N, in increments of 10 N. The voltage measured was plotted versus force. A linear regression was performed to determine the calibration equation. Figure 2.21 shows the load cell calibration.

In addition to the sensor calibration, a relationship between input voltage and current output needed to be established. Each motor driver had a current monitor, providing a way to measure current. Current was represented by a voltage and multiplied by a conversion factor. The conversion factor is specified by the manufacturer. The

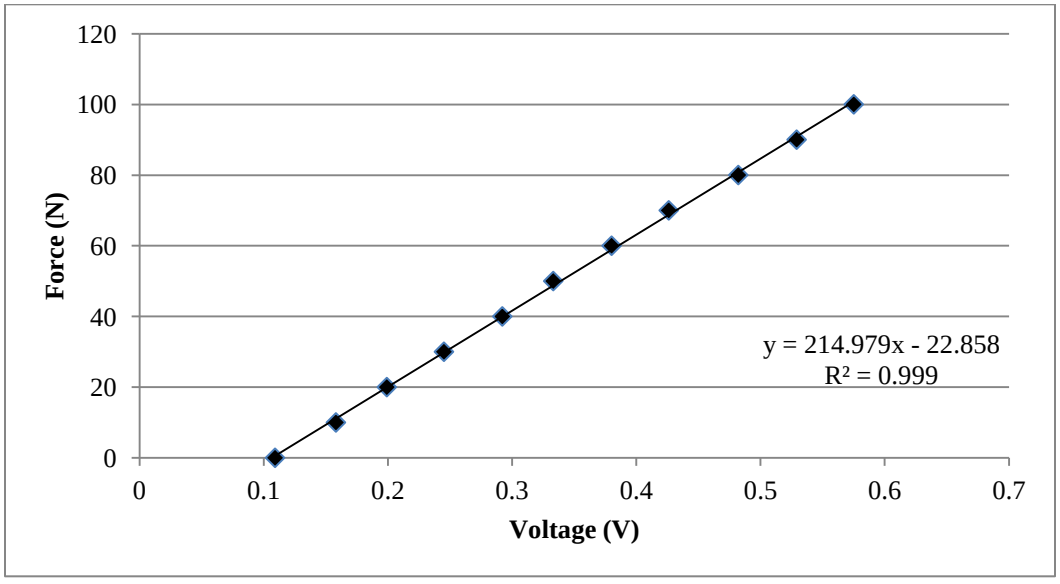

Figure 2.21: Load Cell Calibration

calibration was performed by supplying five different voltages to the driver and using the current monitor to measure current, while keeping the motor stalled. Only relatively small voltages were chosen because of potential difficulty in keeping the motor stalled, since torque is directly related to the current being supplied. The data were graphed and the calibration was obtained by applying a linear fit, contained in Figure 2.22. The calibration equations and R^2 values have been included in both load cell and support motor driver calibration graphs. The y-intercept was excluded in the VI because it was very small.

2.7 Problems and Sources of Error

Throughout the design and testing of the controls, several problems and sources of error were encountered. Two of the largest were friction and mechanical vibration. Both are covered in the following sections.

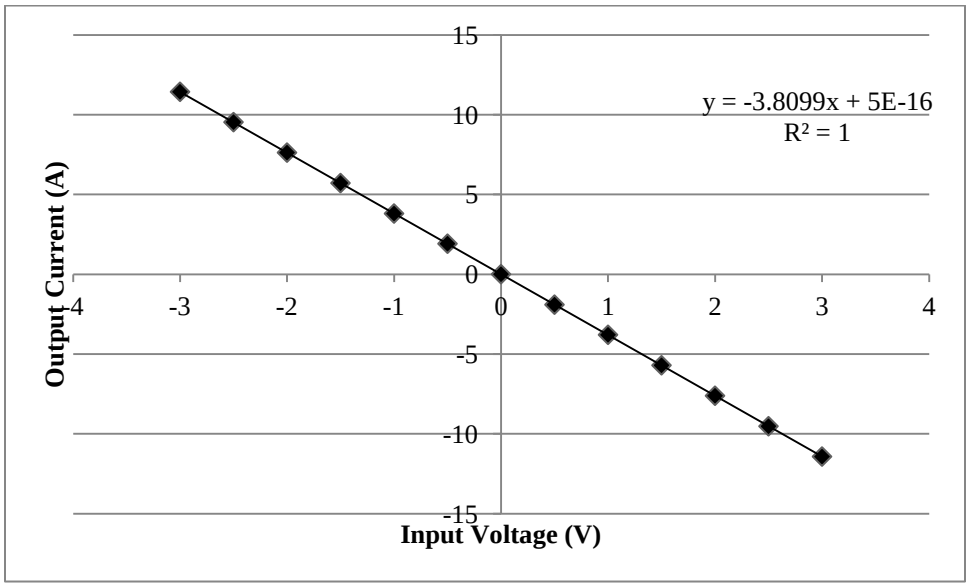

Figure 2.22: Support Motor Driver Calibration

2.7.1 Friction

Initially friction in both drive trains was neglected. However as research progressed, it was found to be a significant source of error. Friction in the torso drive train was measured by lifting the torso slowly using the support. The torso angle and force measured by the load cell were recorded. Force was changed to torque by multiplying the force by the distance between the waist shaft (point of rotation) and load cell. In order to get torque due to friction, the torso's weight was subtracted. The remaining torque was attributed to frictional losses. Torque was plotted versus angle and a polynomial fit was used to obtain an equation for friction, as a function of angle. This was repeated a few times to check for consistency. Since the results were similar one trial was chosen and included in the support control algorithm. Figure 2.23 shows the data recorded (solid line) and polynomial fit line (dashed line). Friction needed to be taken into account by the support control because it affects the torque, which should be measured by the load cell.

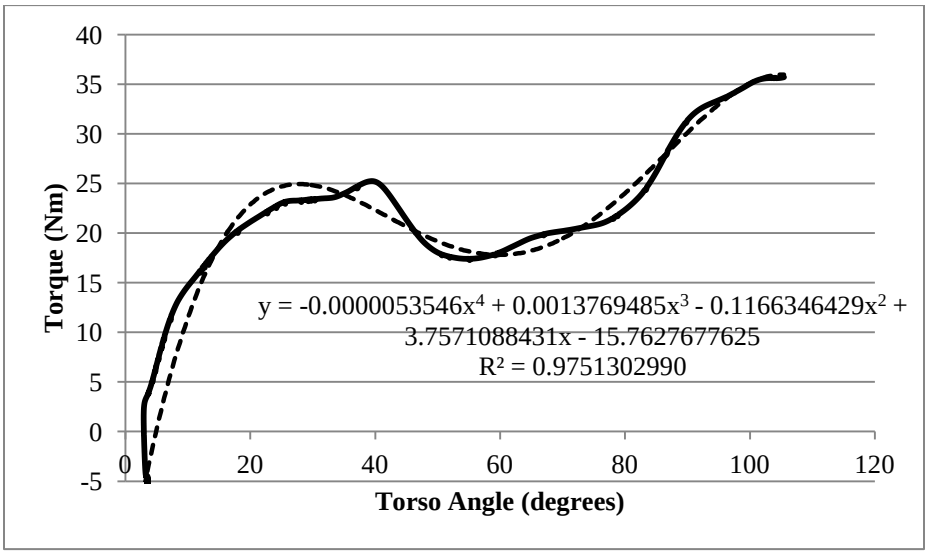

Figure 2.23: Friction vs. Torso Angle

2.8 Mechanical Vibration

Mechanical vibration due to the sprockets and chains may have affected the response of the system. Data were collected to show the vibration by recording the load cell measurement while gravity was pulling the torso down. The back electromotive force (emf) of the torso motor was used to keep a uniform speed. Figure 2.24 is a graph of these data. Notice between 65 and 95 degrees, the vibration decreases. This is likely due to warping of the sprockets. Data could not be collected until the torso was approximately 35 degrees from vertical, because the weight of the torso was unable to overcome friction, back emf, and the torsion spring.

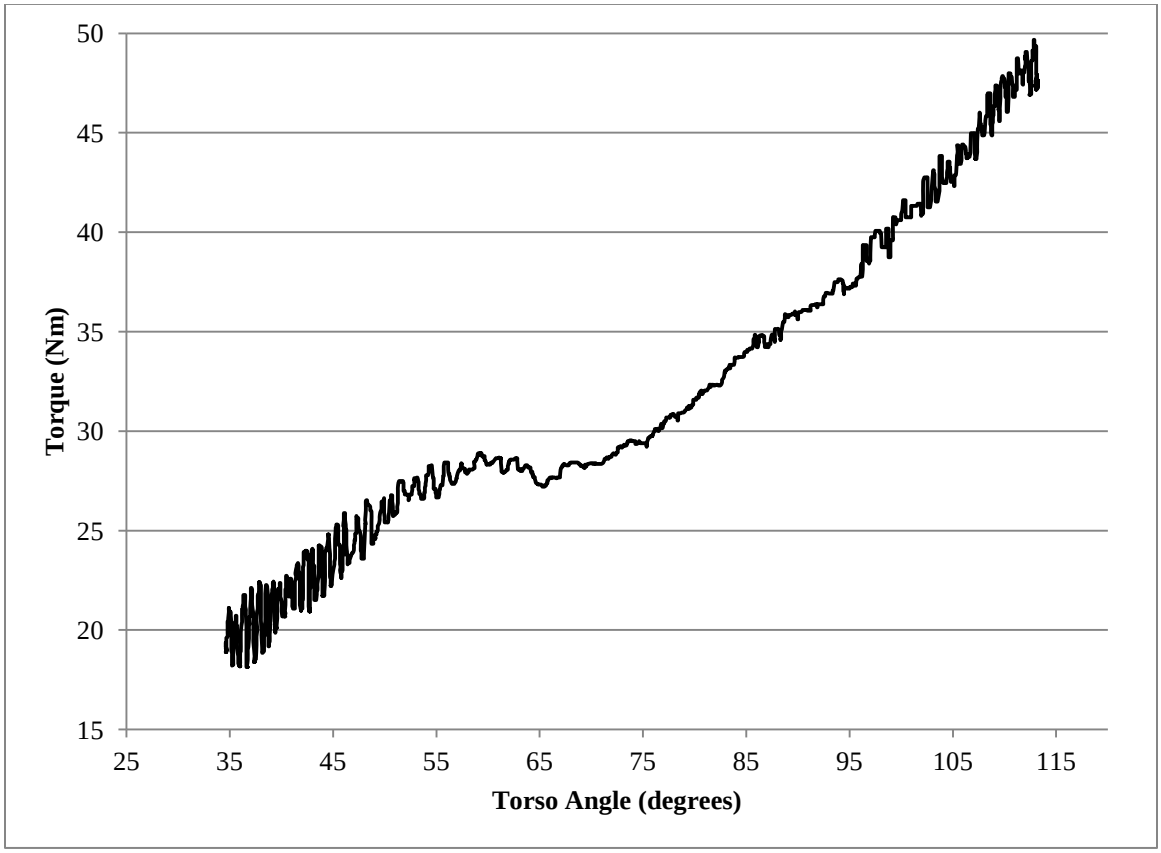

Figure 2.24: Torso Angle vs. Measured Torque (Mechanical Vibration)

2.9 Experimental Design

This section describes the experiment to test if the support control was working properly. Motion capture data collected previously were used to control the torso, in order to better simulate lifting. The purpose of the experiment is to test if the support has an effect on the torso's trajectory, is applying the desired amount of torque (measured torque), and if the torque produced by the torso motor to move through the trajectory is reduced. Ten different percentages of assist, ranging from 0 to 100%, were used with each dataset. Ten percent assist was not included in the analysis because the support had difficulty maintaining contact with the torso because such a small amount of support was needed. For the case of 0% support, the spring was disconnected from the system and the support motor was not used (Figure 2.25).

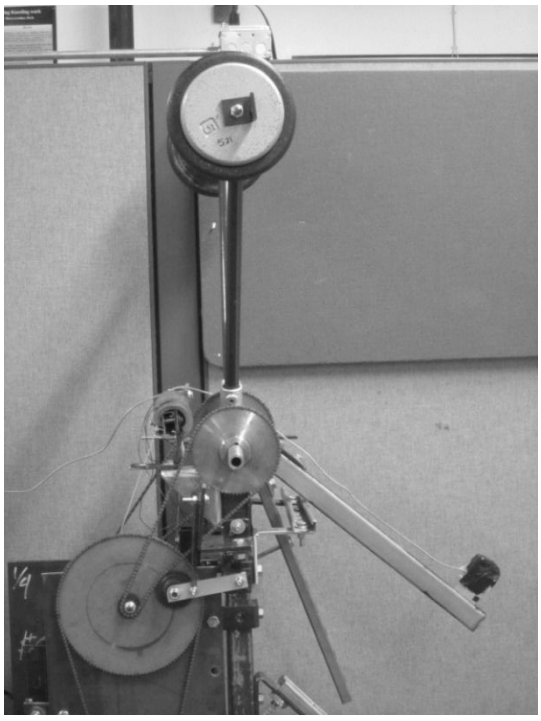

Figure 2.25: Support Position for Trials with No Assist

The following is a list of the data collected for each trial.

- Time
- Target angle
- Torso angle
- Support angle
- Predicted torque
- Target Torque
- Measured torque
- Torso motor torque
- Support motor torque

The null hypothesis for the torso's trajectory is defined as

$$H_0: \mu_1 = \mu_2 = \mu_3 = \mu_4 = \mu_5 = \mu_6 = \mu_7 = \mu_8 = \mu_9 = \mu_{10}$$

where μ_1 is the mean torso angle trajectory for no assist and μ_2 to μ_{10} is the torso angle trajectory when supported by 20 to 100% of assist. The null hypothesis for the measured torque is defined as

$$H_1: \eta_1 = \eta_2 = \eta_3 = \eta_4 = \eta_5 = \eta_6 = \eta_7 = \eta_8 = \eta_9 = \eta_{10}$$

where η_1 is the measured torque for no assist and η_2 to η_{10} is the measured torque when supported by 20 to 100% of assist. The null hypothesis for the measured torque is defined as

$$H_2: \psi_1 = \psi_2 = \psi_3 = \psi_4 = \psi_5 = \psi_6 = \psi_7 = \psi_8 = \psi_9 = \psi_{10}$$

where ψ_1 is the mean torso motor torque for no assist and ψ_2 to ψ_{10} is the mean torso motor torque when supported by 20 to 100% of assist.

To test these effects, the torso control is given new target angle after at least 10 ms had passed since the previous target angle was given. Three different trajectories were chosen (see Figure 2.26, Figure 2.27, and Figure 2.28).

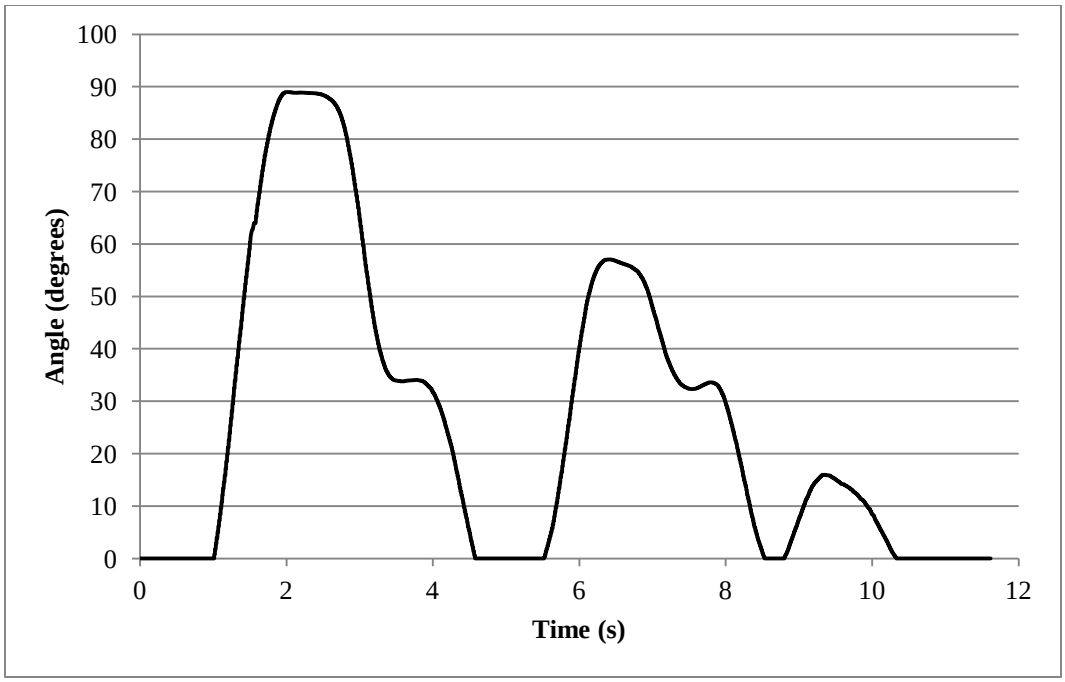

Figure 2.26: Multiple Lifts with Pauses Trajectory

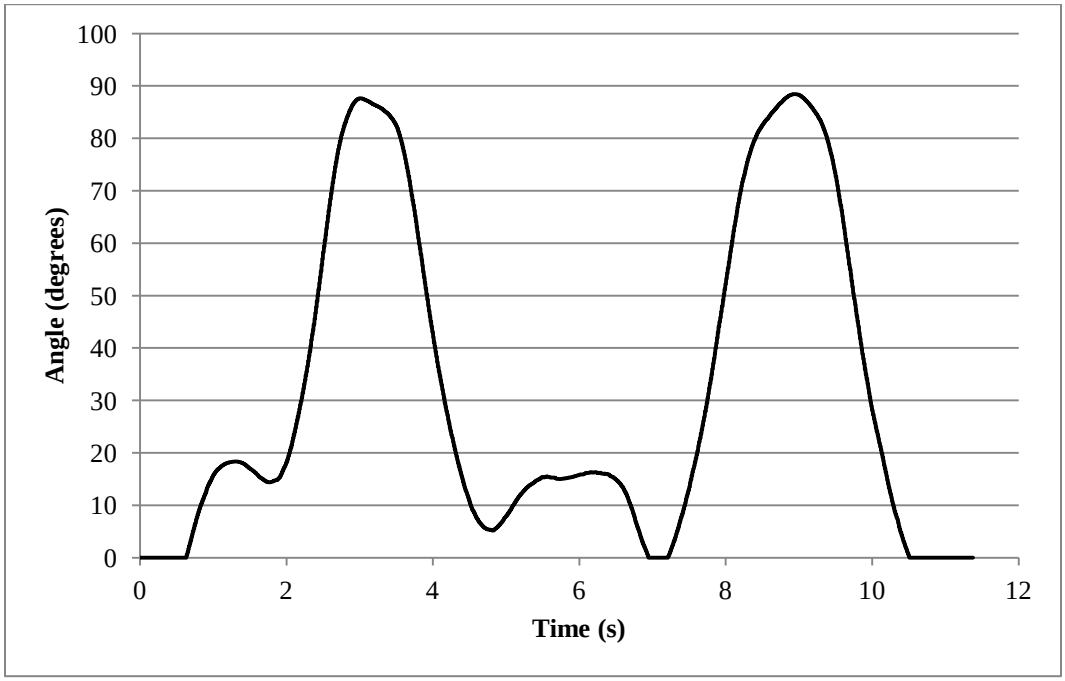

Figure 2.27: Multiple Lifts Trajectory

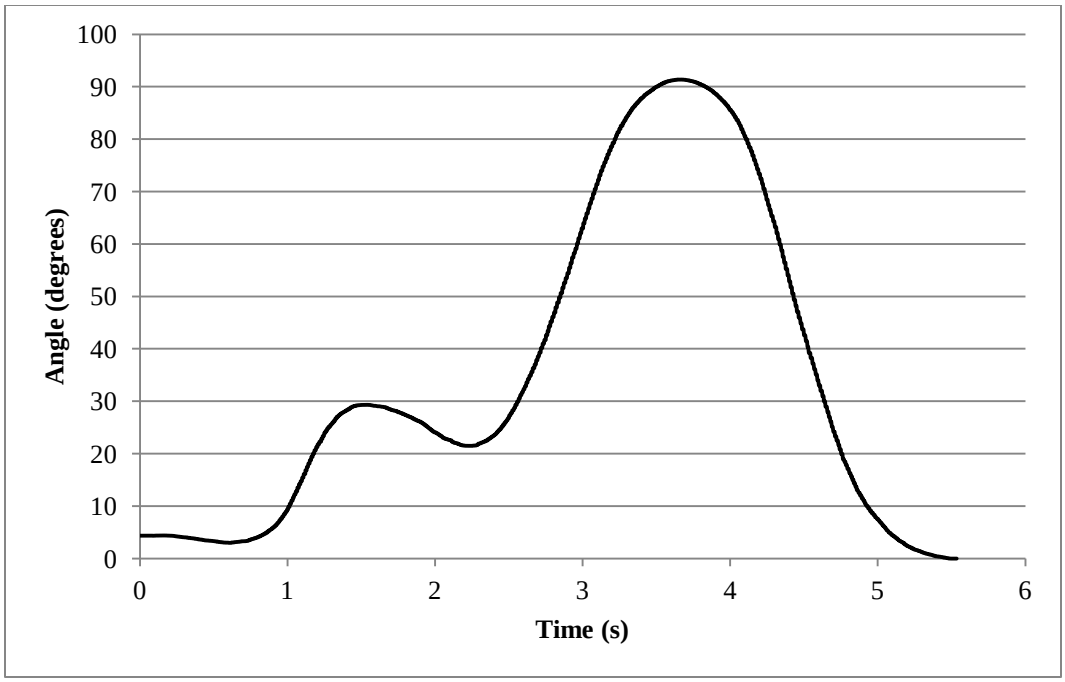

Figure 2.28: Single Lower Trajectory

The first trajectory consisted of multiple lifts with pauses mid-lift. The next trajectory again had multiple lifts but did not have any pauses. The final trajectory was a single lower and performed more slowly than the others. Any negative angles in a trajectory were set to zero degrees for the test. The data were collected using the same VI as the control system. Data were collected from the time when the torso reached the first angle in the trajectory array until it was given the last target angle.

2.9.1 Trajectory Creation

The trajectories used for testing were derived from data collected with an 8 camera Vicon Nexus (Vicon, Centennial CO) system and a custom marker-set. Markers were placed on the C7 vertebrae, sternum, shoulders, upper arms, elbows, wrist, hand, upper legs, and knees. After the trials were processed using the software, the coordinates

for each marker were exported into a data text file. The coordinates, in the sagittal plane, for the right and left anterior superior iliac spine (RASIS and LASIS, respectively) and the C7 vertebrae were used to determine the torso angle (Figure 2.29). The torso angle was found by averaging the RASIS and LASIS coordinates and subtracting them from the coordinates for the C7 vertebrae. The inverse tangent function was used to find the angle in degrees (Figure 2.30).

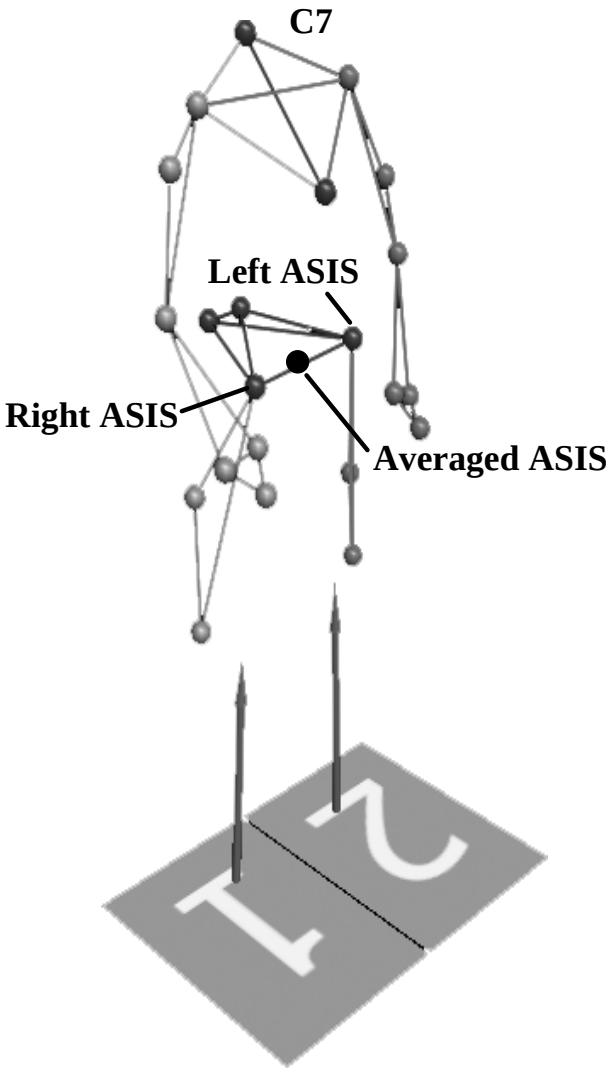

Figure 2.29: Marker Locations

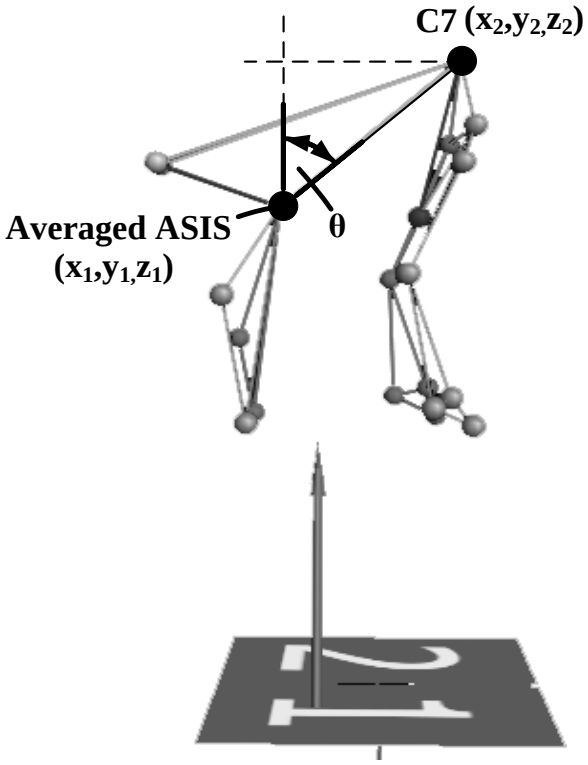

Figure 2.30: Torso Angle

3. RESULTS

3.1 Angular Position

The trajectories for all levels of assist were compared to the trajectory with no assist. The correlations presented in this section are between no assist and each level of assist, along with the mean differences. Table 3.1, Table 3.2, and Table 3.3 contain the mean torso angle, correlation, and mean difference for each assist level. The mean difference is the difference between the average torso angle for no assist and each level of assist. The mean difference for each assist level, between trajectories, is similar. The t-values in each table indicate there was a statistically significant difference for each trajectory between no assist and all assist levels ($t < 0.0001$). However, there was a high correlation between no assist and each assist level for all three trajectories.

Table 3.1: Multiple Lifts with Pauses Trajectory Statistics Summary

Percent Assist	Mean Angle ± *SD* (Degrees)	Mean Difference (Degrees)	Correlation	*t*
0% Assist	32.0 ± 30.8	REF	REF	REF
20% Assist	30.4 ± 30.4	-1.6	1.0	<0.0001
30% Assist	30.4 ± 29.8	-1.7	1.0	<0.0001
40% Assist	30.2 ± 29.6	-1.9	1.0	<0.0001
50% Assist	29.2 ± 29.4	-2.8	1.0	<0.0001
60% Assist	29.1 ± 29.2	-2.9	1.0	<0.0001
70% Assist	29.1 ± 29.0	-2.9	1.0	<0.0001
80% Assist	28.6 ± 28.8	-3.4	1.0	<0.0001
90% Assist	28.5 ± 28.7	-3.5	1.0	<0.0001
100% Assist	28.2 ± 28.4	-3.8	1.0	<0.0001

Table 3.2: Multiple Lifts Trajectory Statistics Summary

Percent Assist	**Mean Angle ± *SD* (Degrees)**	**Mean Difference (Degrees)**	**Correlation**	***t***
0% Assist	36.3 ± 31.9	REF	REF	REF
20% Assist	35.1 ± 31.6	-1.3	1.0	<0.0001
30% Assist	34.5 ± 31.4	-1.8	1.0	<0.0001
40% Assist	34.4 ± 31.2	-1.9	1.0	<0.0001
50% Assist	33.8 ± 31.0	-2.5	1.0	<0.0001
60% Assist	32.3 ± 31.0	-4.1	0.9	<0.0001
70% Assist	33.1 ± 30.7	-3.2	1.0	<0.0001
80% Assist	32.8 ± 30.4	-3.5	1.0	<0.0001
90% Assist	32.5 ± 30.2	-3.8	1.0	<0.0001
100% Assist	32.4 ± 30.0	-4.0	1.0	<0.0001

Table 3.3: Single Lower Trajectory Statistics Summary

Percent Assist	**Mean Angle ± *SD* (Degrees)**	**Mean Difference (Degrees)**	**Correlation**	***t***
0% Assist	38.2 ± 31.4	REF	REF	REF
20% Assist	37.0 ± 31.3	-1.2	1.0	<0.0001
30% Assist	36.8 ± 31.0	-1.5	1.0	<0.0001
40% Assist	36.5 ± 30.8	-1.7	1.0	<0.0001
50% Assist	36.0 ± 30.6	-2.3	1.0	<0.0001
60% Assist	35.5 ± 30.5	-2.8	1.0	<0.0001
70% Assist	35.3 ± 30.1	-3.0	1.0	<0.0001
80% Assist	34.9 ± 30.1	-3.3	1.0	<0.0001
90% Assist	34.6 ± 29.9	-3.6	1.0	<0.0001
100% Assist	34.1 ± 29.3	-4.2	1.0	<0.0001

Although a statistical difference was found, the measured trajectories were similar graphically (see Figure 3.1, Figure 3.2, and Figure 3.3). For reference, the target trajectory was included in these graphs. Because there was a time lag between the target trajectories and when torso responded, the target trajectory was shifted to the right to make comparing the target and measured trajectories more convenient. The graphs seem to indicate that the torso followed the target trajectory more closely as the assist level increased. Close to maximum torso extension (the torso was near horizontal), the torso control would overshoot the trajectory when it was unassisted (0% assist). The overshoot appears to be consistent and does not vary much with a change in target trajectory. This overshooting only seems to be affected by the change in assist.

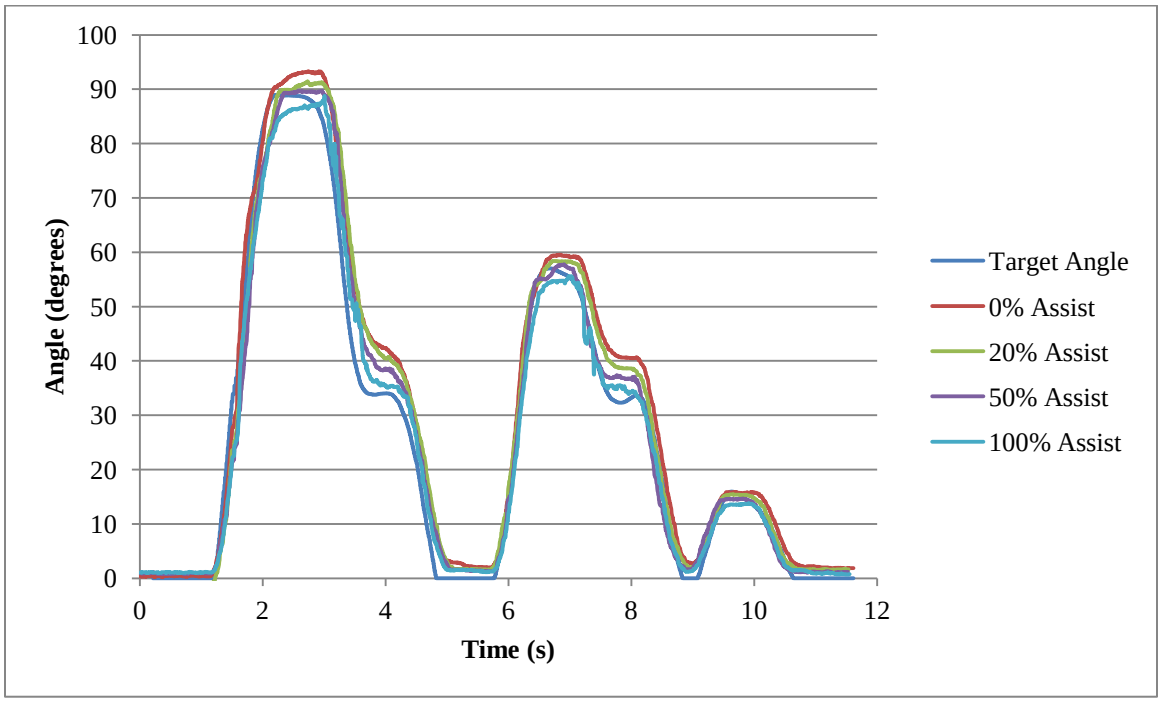

Figure 3.1: Multiple Lifts with Pauses Trajectory Torso Angle vs. Time for Selected Levels of Assist

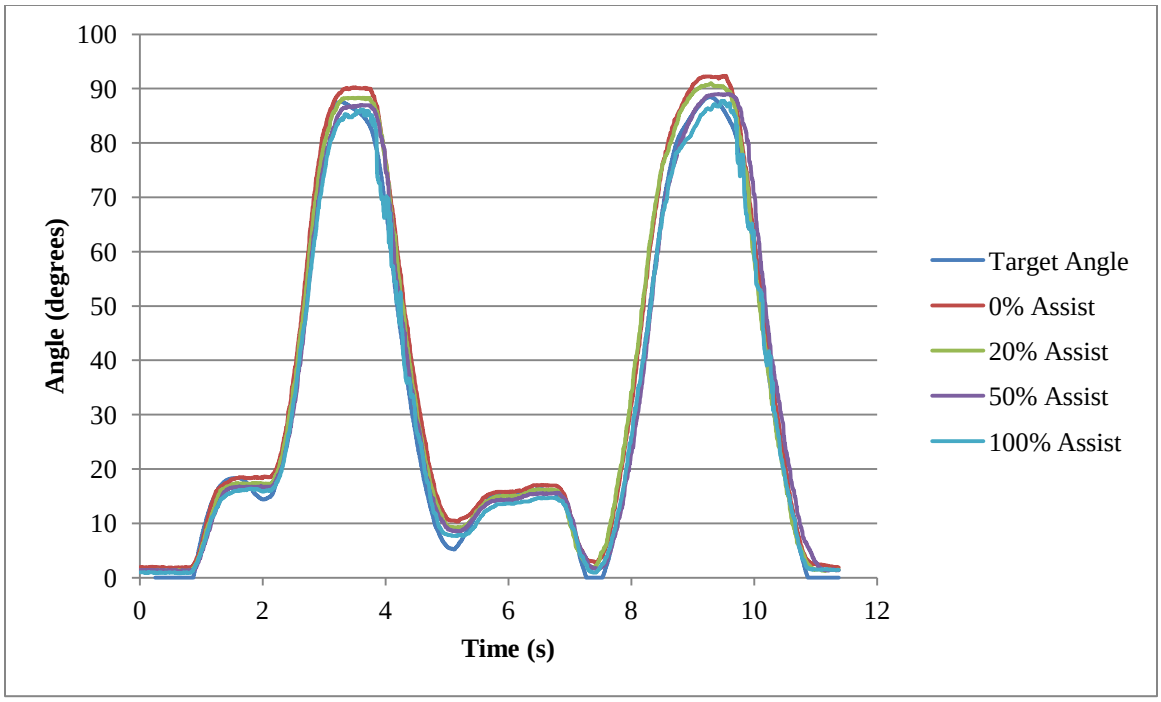

Figure 3.2: Multiple Lifts Trajectory Torso Angle vs. Time for Selected Levels of Assist

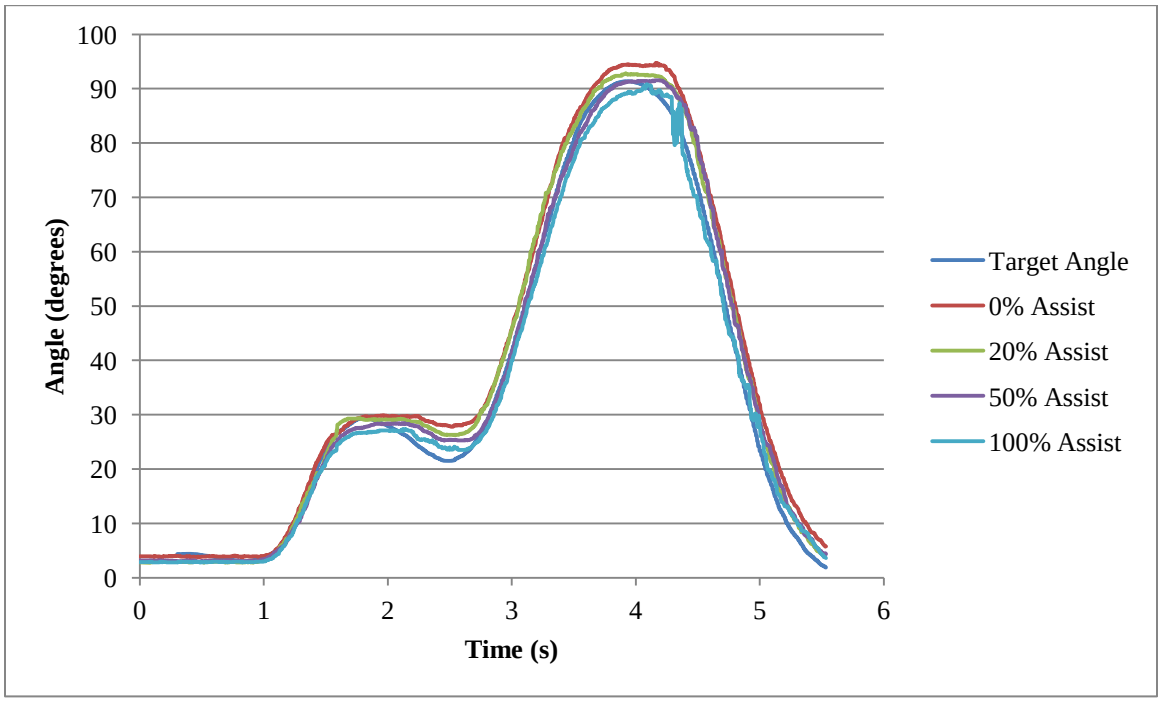

Figure 3.3: Single Lower Trajectory Torso Angle vs. Time for Selected Levels of Assist

Looking at the graphs above (Figure 3.1, Figure 3.2, and Figure 3.3), large differences in trajectories occur during a sudden change in the trajectory, such as just before a pause mid-lift. Figure 3.4 illustrates an example of a pause. The pause occurs within the black box. The torso's trajectory appears to better match the target trajectory as the assist level increases, as there is less overshoot. This implies that torso motor was better able move the torso through the transitions, with the additional assistance. After the transition, the trajectories appear to cluster together implying the torso followed a similar path when assisted. When the torso was fully assisted (100% assist), the trajectory appears to have more variation than the others, indicated by the fluctuations in the graphs. As the multiple lifts trajectory does not have any pauses mid-lift, the torso appeared to follow that target trajectory the best.

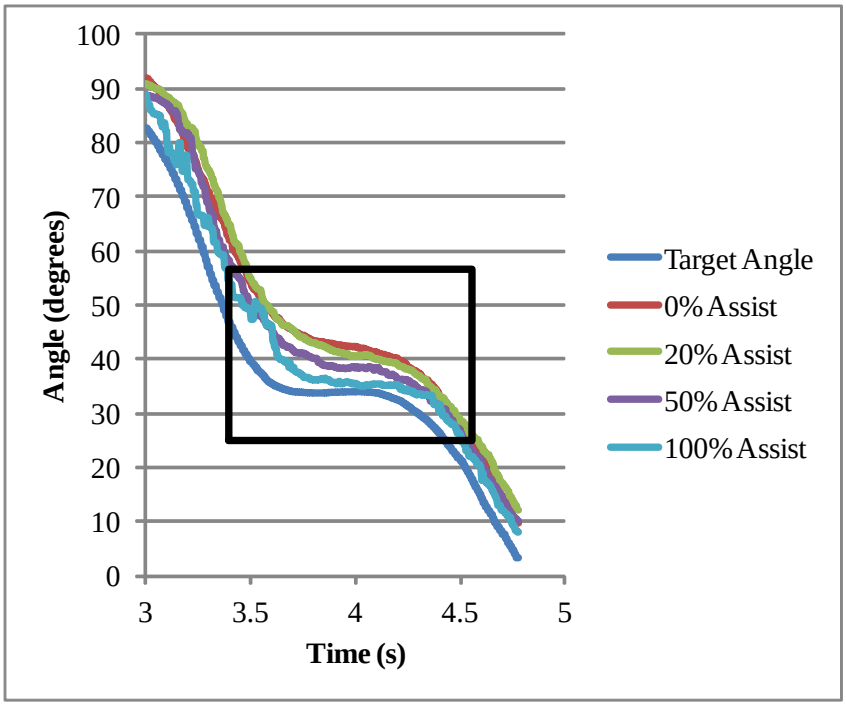

Figure 3.4: Pause in Torso Movement

3.2 Load Cell

The statistics comparing the data collected from the load cell to the desired value indicate that there was no statistical difference. The t-values for all trials were greater than 0.05 (see Table 3.4, Table 3.5, and Table 3.6). Since there was no statistical significance detected, it is likely that the support functioned as desired and the proper amount of force was applied at the shoulder. The torques in these tables can be converted to a close approximation of force applied to the torso by multiplying by 2. The mean difference in these tables is the difference between the target torque mean and measured torque mean, for each level of assist. The mean differences are close to zero. The following graphs show the measured torque vs. the target torque for certain assist levels (Figure 3.5, Figure 3.6, and Figure 3.7). These were included for a visual comparison.

Table 3.4: Multiple Lifts with Pauses Trajectory Torque Statistics Summary

Percent Assist	**Target Torque Mean ± *SD* (Nm)**	**Measured Torque Mean ± *SD* (Nm)**	**Mean Difference (Nm)**	***t***
20% Assist	10.81 ± 7.91	10.76 ± 7.84	-0.05	0.32
30% Assist	14.42 ± 10.75	14.37 ± 10.62	-0.05	0.35
40% Assist	17.82 ± 13.86	17.83 ± 13.63	0.01	0.86
50% Assist	20.96 ± 16.86	20.96 ± 16.62	0.01	0.92
60% Assist	24.30 ± 19.81	24.29 ± 19.51	-0.01	0.90
70% Assist	27.53 ± 22.87	27.56 ± 22.51	0.03	0.51
80% Assist	30.33 ± 25.68	30.31 ± 25.35	-0.02	0.76
90% Assist	32.46 ± 29.36	32.46 ± 29.18	0.00	0.97
100% Assist	34.40 ± 32.38	34.41 ± 32.11	0.01	0.90

Table 3.5: Multiple Lifts Trajectory Torque Statistics Summary

Percent Assist	Target Torque Mean ± *SD* (Nm)	Measured Torque Mean ± *SD* (Nm)	Mean Difference (Nm)	*t*
20% Assist	11.46 ± 7.51	11.46 ± 7.32	0.00	0.96
30% Assist	15.34 ± 10.49	15.33 ± 10.22	-0.01	0.85
40% Assist	19.04 ± 13.50	19.05 ± 13.15	0.01	0.89
50% Assist	22.54 ± 16.53	22.53 ± 16.15	-0.01	0.73
60% Assist	25.09 ± 20.09	25.11 ± 19.99	0.02	0.85
70% Assist	29.61 ± 22.86	29.60 ± 22.50	-0.01	0.91
80% Assist	32.42 ± 26.05	32.43 ± 25.68	0.01	0.92
90% Assist	35.75 ± 29.09	35.74 ± 28.68	-0.01	0.85
100% Assist	38.34 ± 32.75	38.34 ± 32.16	0.01	0.94

Table 3.6: Single Lower Trajectory Torque Statistics Summary

Percent Assist	Target Torque Mean ± *SD* (Nm)	Measured Torque Mean ± *SD* (Nm)	Mean Difference (Nm)	*t*
20% Assist	12.05 ± 7.52	11.98 ± 7.44	-0.07	0.17
30% Assist	16.55 ± 9.84	16.53 ± 9.67	-0.02	0.71
40% Assist	20.70 ± 13.83	20.58 ± 13.60	-0.12	0.06
50% Assist	24.62 ± 15.52	24.57 ± 15.22	-0.05	0.42
60% Assist	28.51 ± 18.46	28.48 ± 18.14	-0.03	0.58
70% Assist	32.16 ± 21.43	32.09 ± 21.11	-0.08	0.29
80% Assist	35.92 ± 24.36	35.82 ± 24.11	-0.10	0.21
90% Assist	39.42 ± 27.41	39.28 ± 27.48	-0.14	0.31
100% Assist	41.75 ± 30.89	41.78 ± 30.22	0.03	0.76

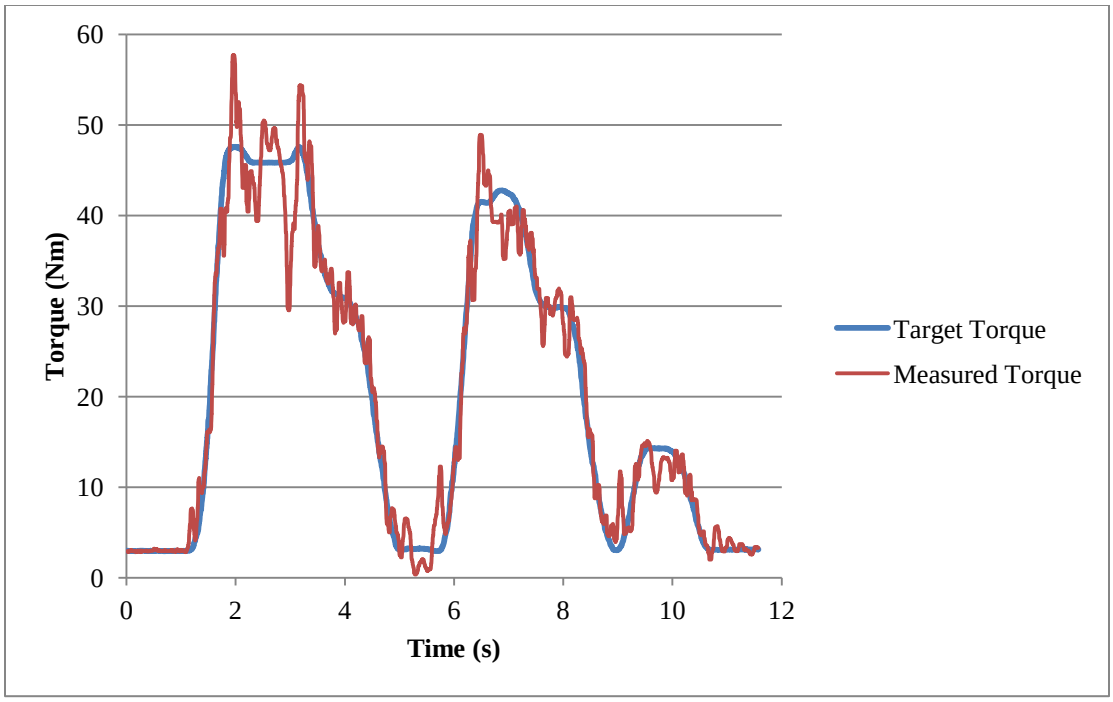

Figure 3.5: Multiple Lifts with Pauses Trajectory - 50% Assist Comparison of Measured Torque and Target Torque

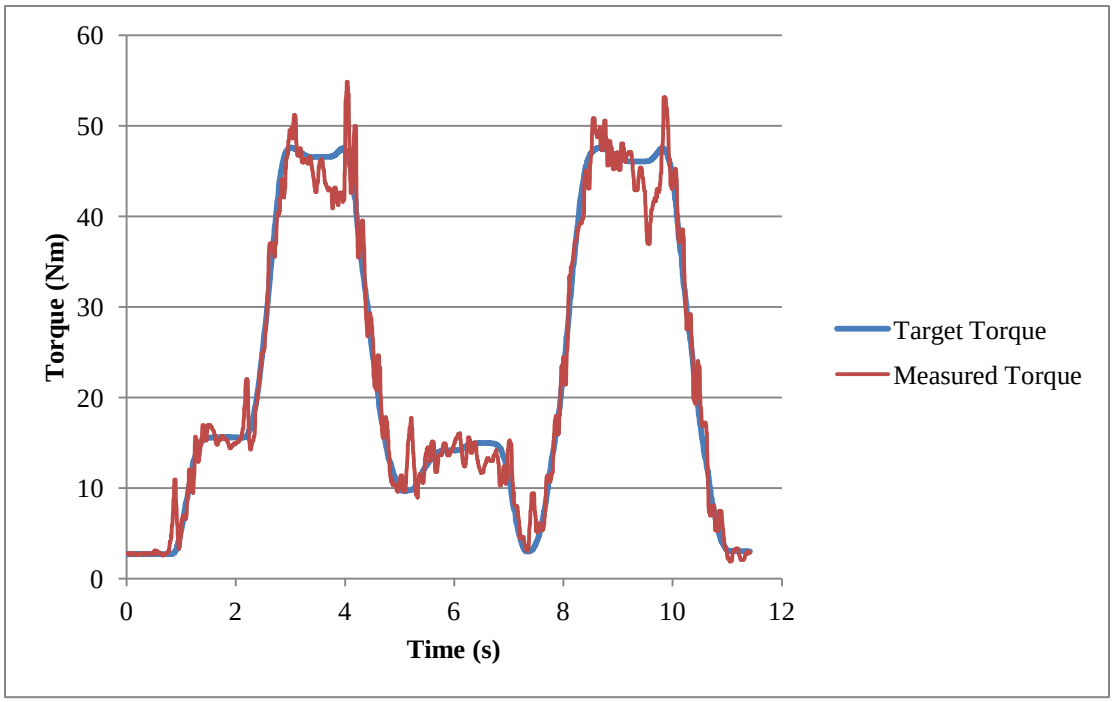

Figure 3.6: Multiple Lifts Trajectory - 50% Assist Comparison of Measured Torque and Target Torque

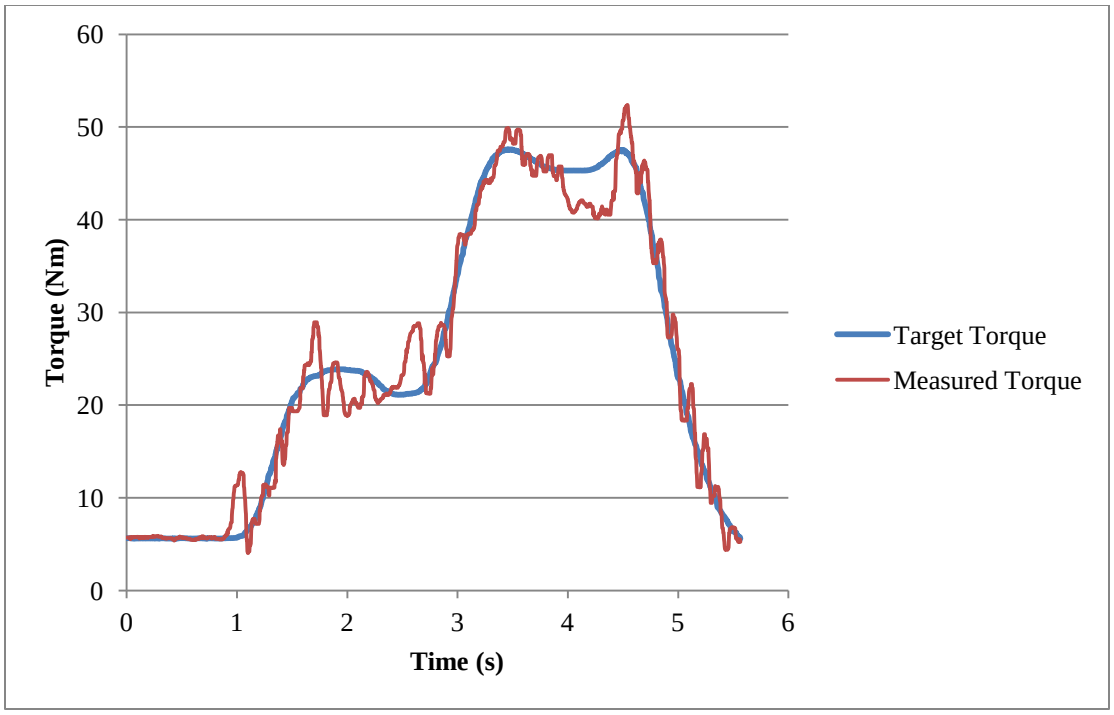

Figure 3.7: Single Lower Trajectory - 50% Assist Comparison of Measured Torque and Target Torque

3.3 Torso Motor Torque

A summary of statistics are included in Table 3.7, Table 3.8, and Table 3.9 for each trajectory. Again the mean difference reported is the difference between the mean torque for each assist level (20 - 100%) and mean torque with no assist. A statistical difference was detected for every trial ($t < 0.0001$). The mean torso motor torque was the largest when the torso was unassisted and the smallest when fully assisted. Also, the mean torso motor torque decreases as the assist level increases, as expected. Graphs of torso motor torque for each trajectory are shown in Figure 3.8, Figure 3.9, and Figure 3.10. The graph shows the torque the motor had to produce was reduced corresponding to the greater assist level. The graphs for the mean torso motor torque for each assist level are located in Figure 3.11, Figure 3.12, and Figure 3.13.

Table 3.7: Multiple Lifts with Pauses Trajectory Torso Motor Torque Statistics Summary

Percent Assist	Mean Torso Motor Torque ± *SD* (Nm)	Mean Difference (Nm)	*t*
0% Assist	39.3 ± 44.9	REF	<0.0001
20% Assist	24.8 ± 43.9	-14.4	<0.0001
30% Assist	24.6 ± 38.5	-14.7	<0.0001
40% Assist	20.8 ± 36.6	-18.4	<0.0001
50% Assist	16.1 ± 33.7	-23.2	<0.0001
60% Assist	13.2 ± 31.4	-26.1	<0.0001
70% Assist	10.3 ± 30.1	-28.9	<0.0001
80% Assist	7.2 ± 27.8	-32.0	<0.0001
90% Assist	4.9 ± 26.4	-34.3	<0.0001
100% Assist	1.9 ± 24.8	-37.4	<0.0001

Table 3.8: Multiple Lifts Trajectory Torso Motor Torque Statistics Summary

Percent Assist	Mean Torso Motor Torque ± *SD* (Nm)	Mean Difference (Nm)	*t*
0% Assist	37.5 ± 42.1	REF	<0.0001
20% Assist	24.3 ± 39.3	-13.1	<0.0001
30% Assist	20.5 ± 36.9	-16.9	<0.0001
40% Assist	17.5 ± 34.8	-20.0	<0.0001
50% Assist	13.3 ± 32.7	-24.2	<0.0001
60% Assist	10.0 ± 29.1	-27.5	<0.0001
70% Assist	6.5 ± 27.9	-31.0	<0.0001
80% Assist	3.3 ± 25.8	-34.2	<0.0001
90% Assist	0.3 ± 24.0	-37.1	<0.0001
100% Assist	-3.4 ± 22.2	-40.9	<0.0001

Table 3.9: Single Lower Trajectory Torso Motor Torque Statistics Summary

Percent Assist	Mean Torso Motor Torque ± *SD* (Nm)	Mean Difference (Nm)	*t*
0% Assist	37.9 ± 42.5	REF	<0.0001
20% Assist	24.3 ± 41.1	-13.6	<0.0001
30% Assist	21.0 ± 37.4	-16.9	<0.0001
40% Assist	17.5 ± 35.1	-20.4	<0.0001
50% Assist	13.9 ± 33.1	-24.0	<0.0001
60% Assist	9.9 ± 31.1	-28.0	<0.0001
70% Assist	6.6 ± 28.2	-31.3	<0.0001
80% Assist	3.1 ± 26.5	-34.8	<0.0001
90% Assist	0.4 ± 24.7	-37.5	<0.0001
100% Assist	-3.2 ± 23.5	-41.2	<0.0001

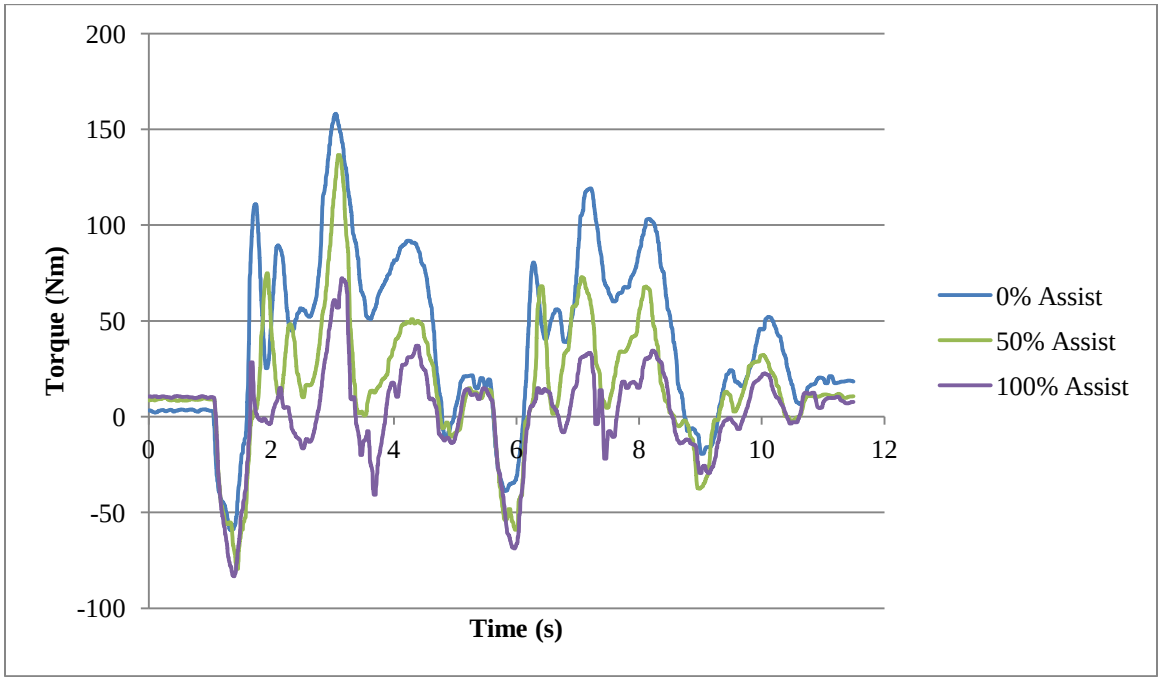

Figure 3.8: Multiple Lifts with Pauses Trajectory Torso Motor Torque for Select Levels of Assist

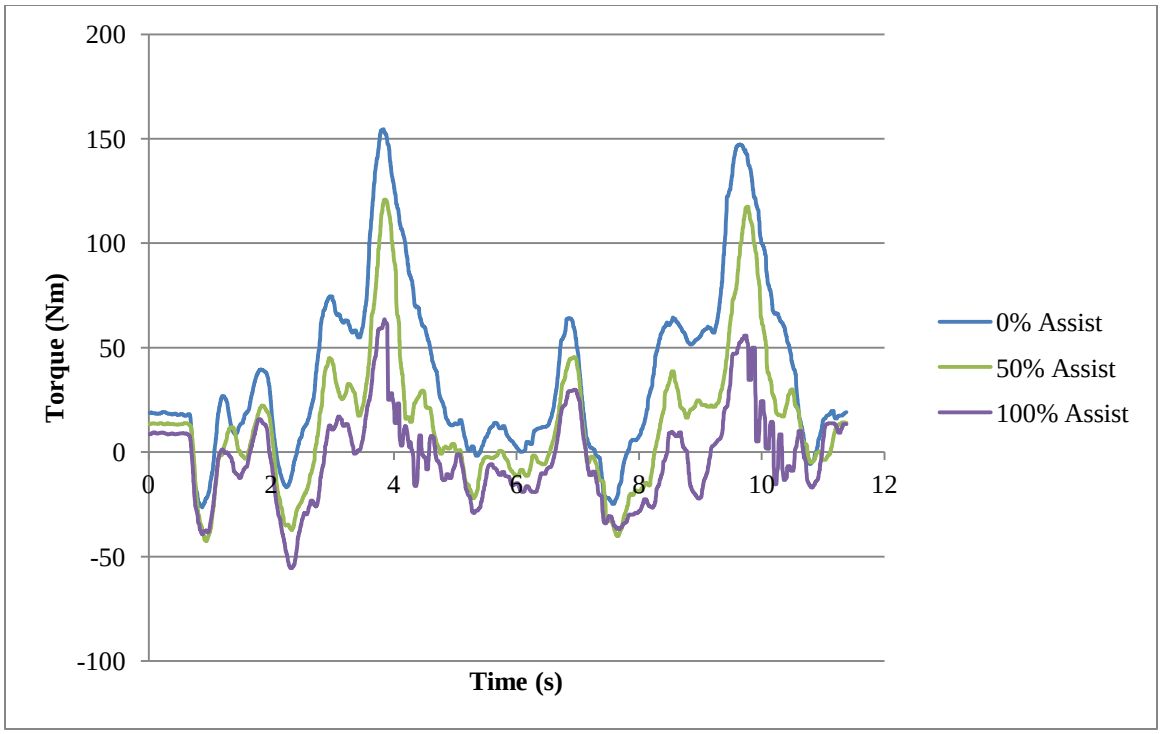

Figure 3.9: Multiple Lifts Trajectory Torso Motor Torque for Select Levels of Assist

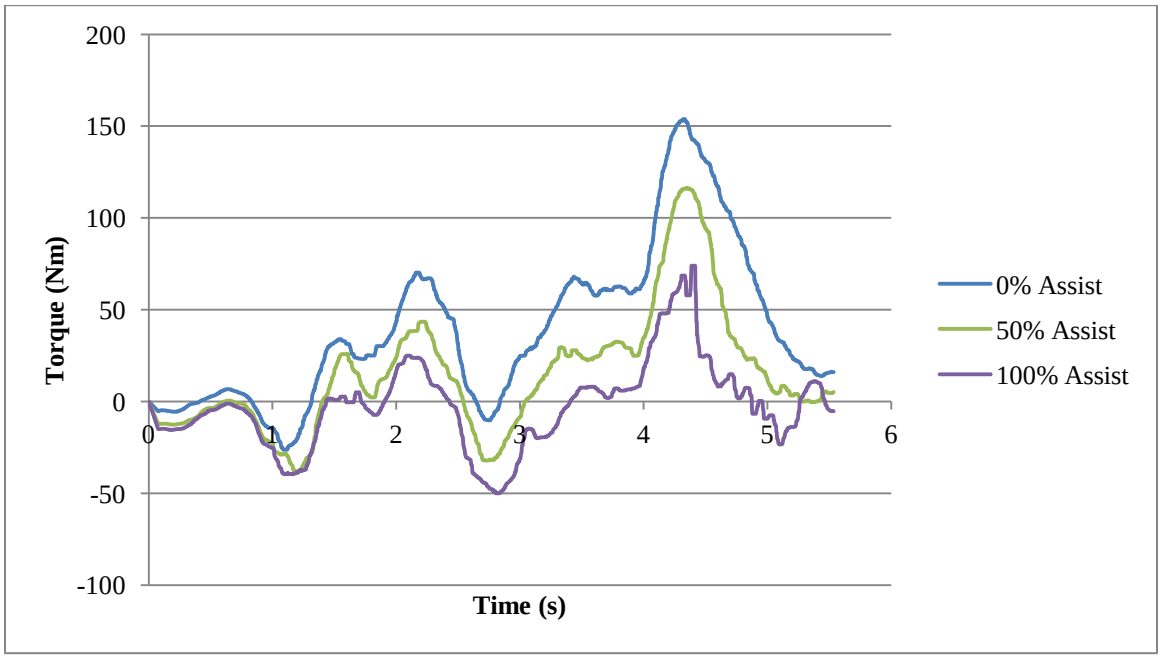

Figure 3.10: Single Lower Trajectory Torso Motor Torque for Select Levels of Assist

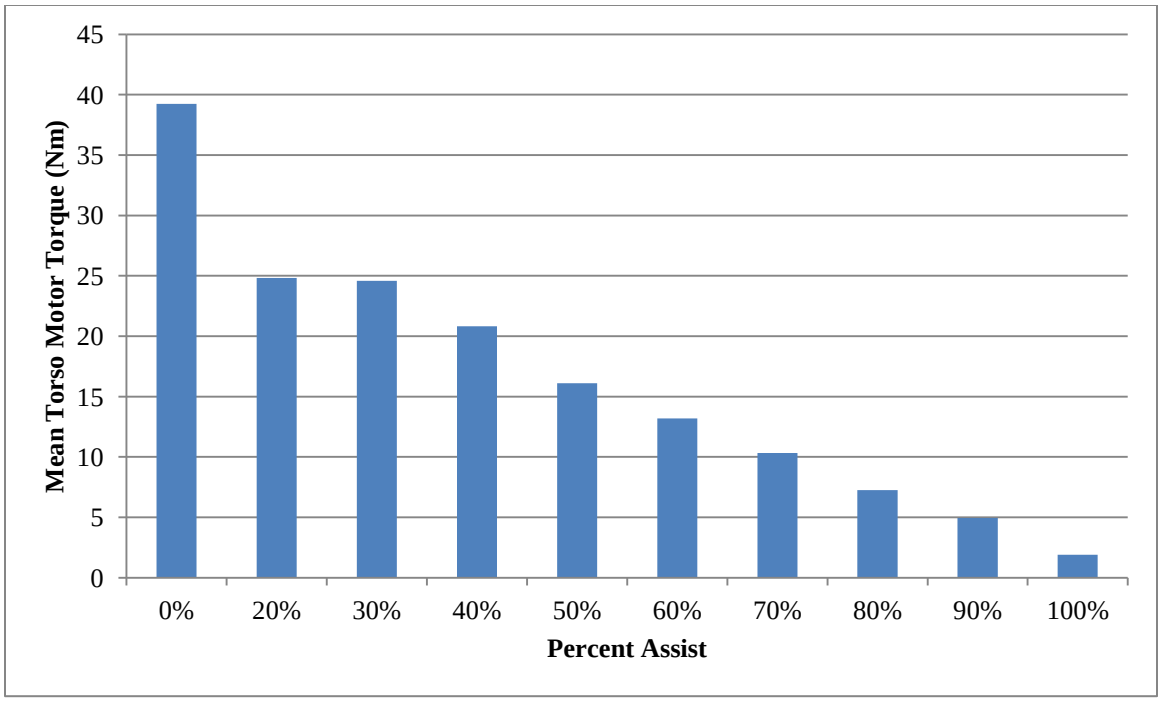

Figure 3.11: Multiple Lifts with Pauses Trajectory Mean Torso Motor Torque by Levels of Assist

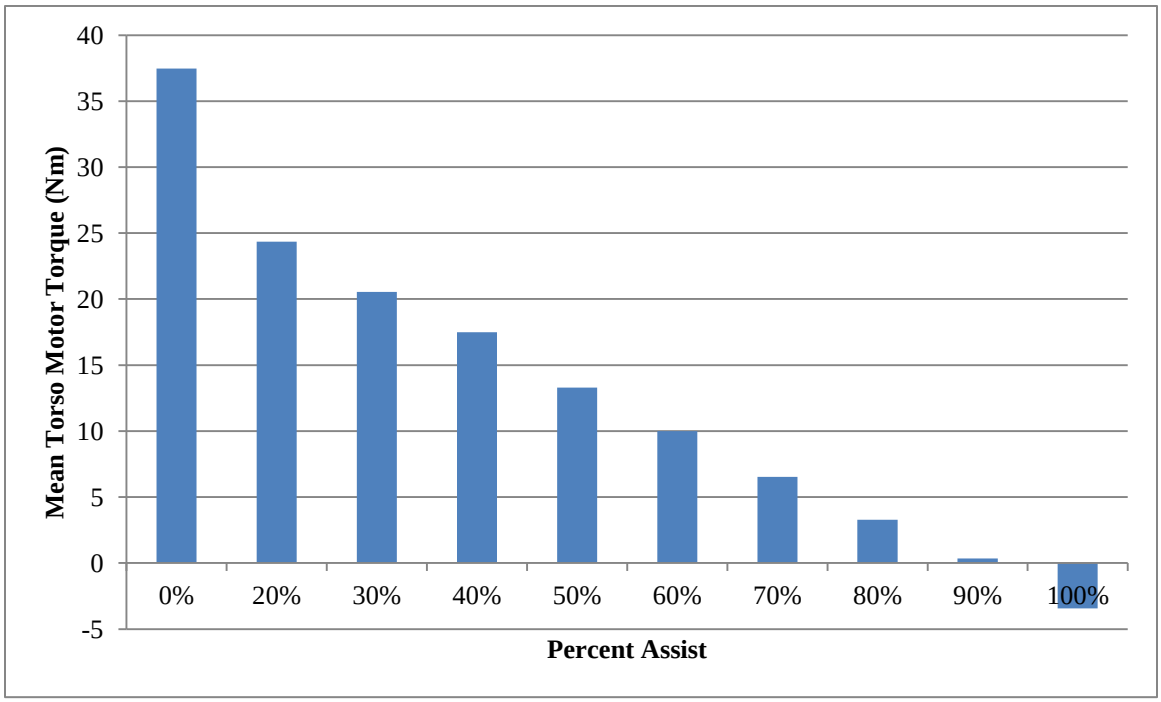

Figure 3.12: Multiple Lifts Trajectory Mean Torso Motor Torque by Levels of Assist

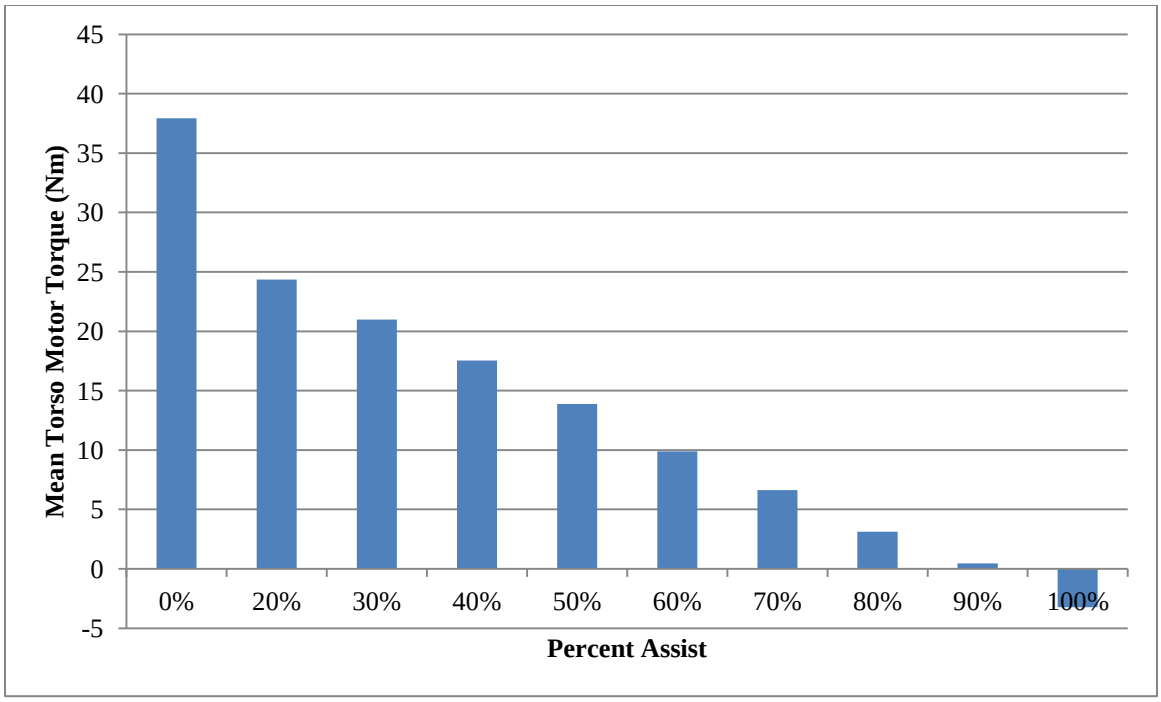

Figure 3.13: Single Lower Trajectory Mean Torso Motor Torque by Levels of Assist

Figure 3.14, Figure 3.15, and Figure 3.16 contain graphs of the percent difference between the mean torso motor torque with no assist and each level of assist. The percent difference was calculated using Equation 3.1 where $\bar{\tau}_0$ is the mean torso motor torque with no assist and $\bar{\tau}_X$ is the mean torso motor torque for each level of assist.

$$\text{Percent Difference} = \left(\frac{\bar{\tau}_0 - \bar{\tau}_x}{\bar{\tau}_0}\right) 100 \qquad \text{Equation 3.1}$$

In Figure 3.12 and Figure 3.13 the percent difference is greater than 100, when the support was providing full assistance. Obviously this is because the mean for the multiple lifts and single lower trajectories were negative, for the 100% assist trial. This means that more negative torque was applied by the torso motor during these trials than positive torque. Negative torque is discussed in the next chapter.

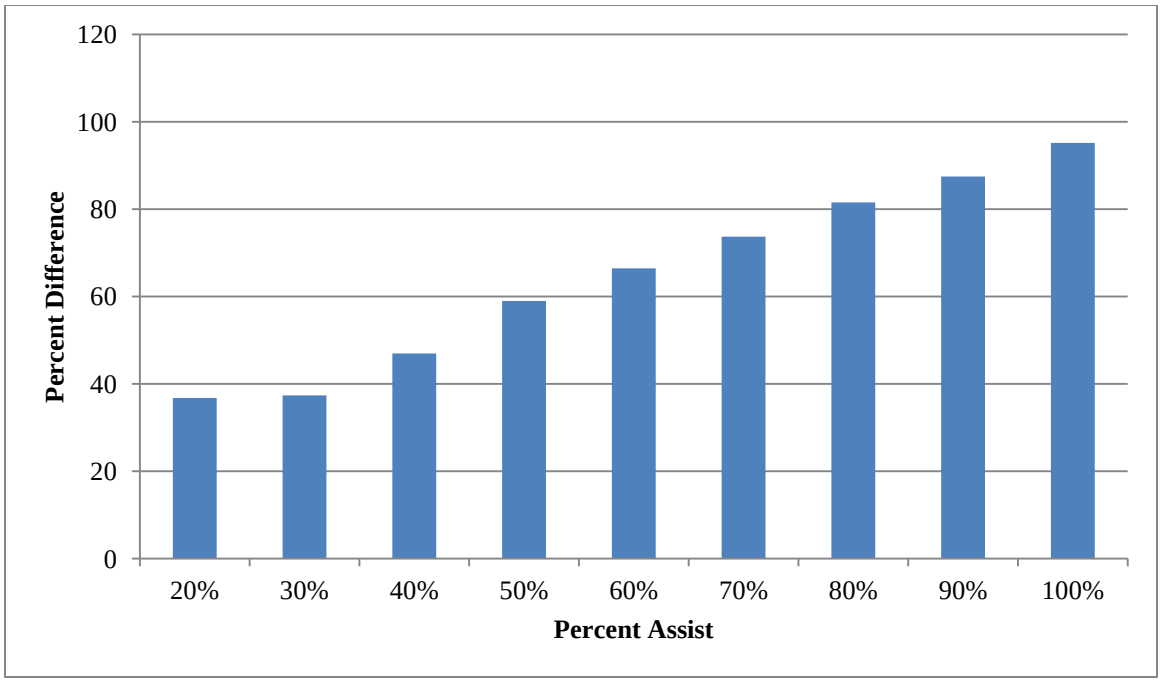

Figure 3.14: Multiple Lifts with Pauses Trajectory Torso Motor Torque Percent Difference by Level of Assist

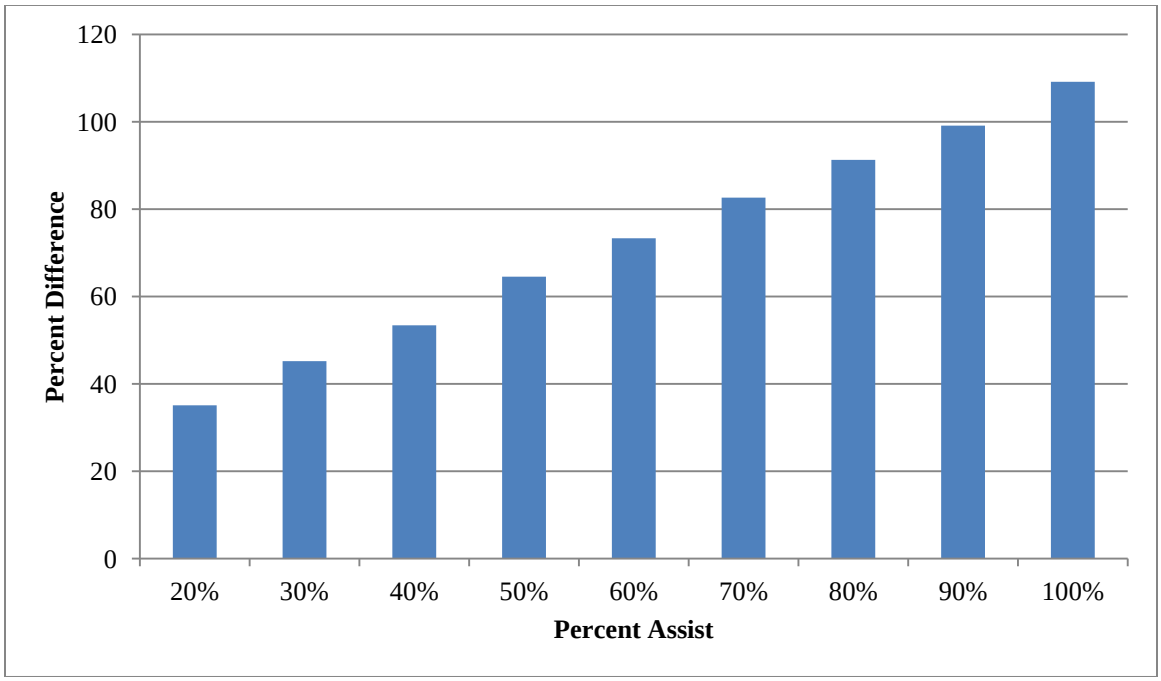

Figure 3.15: Multiple Lifts Trajectory Torso Motor Torque Percent Difference by Level of Assist

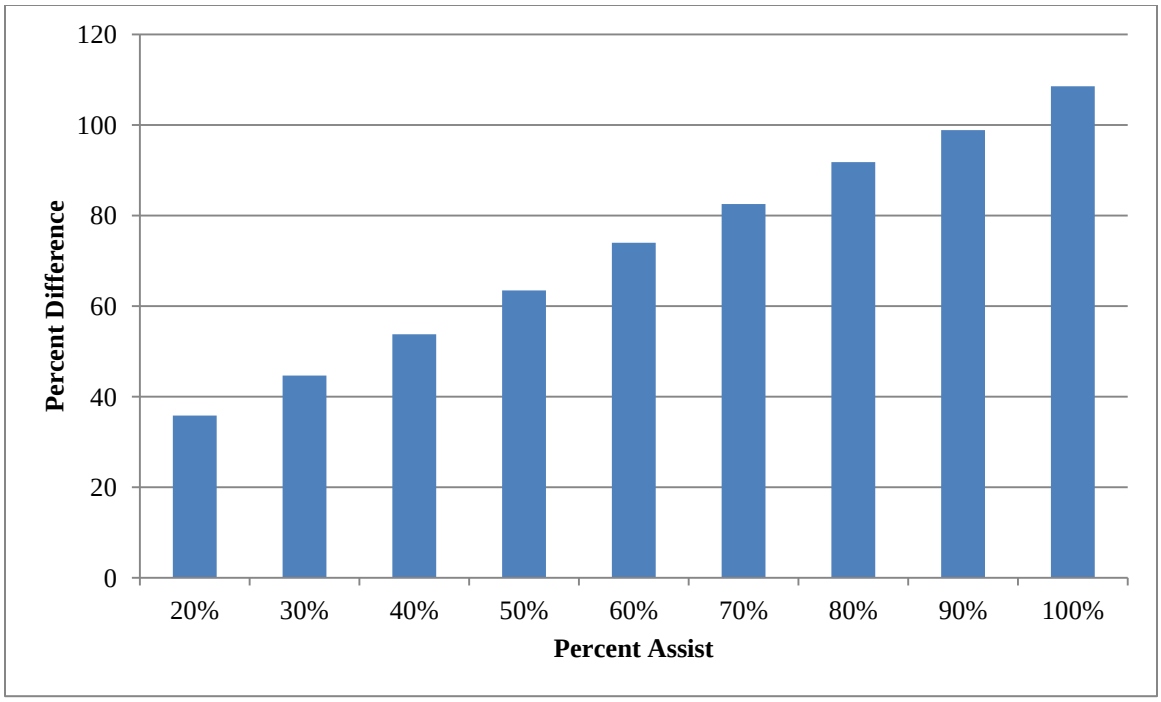

Figure 3.16: Single Lower Trajectory Torso Motor Torque Percent Difference by Level of Assist

4. DISCUSSION

4.1 Angular Trajectory

Although the statistical analysis indicates there is a significant difference between trajectories, the overlapping trajectories shown in Figure 3.1, Figure 3.2, and Figure 3.3, indicate that these values may not be practically different. It is possible a statistical significance was detected because of the large number of samples and low standard error. Looking at the graphs, the largest differences in trajectories occur during a sudden change in position, such as just before a pause. As the multiple lifts trajectory does not have any pauses mid-lift, the torso appeared to follow that trajectory the best.

4.2 Load Cell

The measurements taken from the load cell indicate that the support is providing the desired amount of assist. The measured torque fluctuated compared to the target torque. The small mean difference reported in Table 3.4, Table 3.5, and Table 3.6 implies that there was a nearly equal amount of positive and negative torque overshoot. This is largely a function of the control system gains and system parameters that could be improved with future iterations.

The largest peaks and valleys in the measured torque graph typically occur during transition periods of torso movement. These periods take place at the end of torso flexion. During these times the support had the most difficulty applying the desired

amount of assist. Often the support over corrected and would overshoot or undershoot the target torque (see Figure 4.1). The largest peak in this figure is approximately 10 Nm (or about 20 N of force) above the desired value. A potential improvement to the control would be to increase the derivative gain in the PID control. This would add damping to the system, which would reduce the amount of overshoot and undershoot around the target. As a result it should also reduce the instability as the torso transitions from motion to stationary position and the support control compensates for this change. However, the derivative gain is sensitive to noise and can add instability if too large. Through trial and error the gain was increased in the PID control as much as possible without causing instability that can occur because of this sensitivity. Peaks also occurred at the start of torso flexion, shown in Figure 4.2.

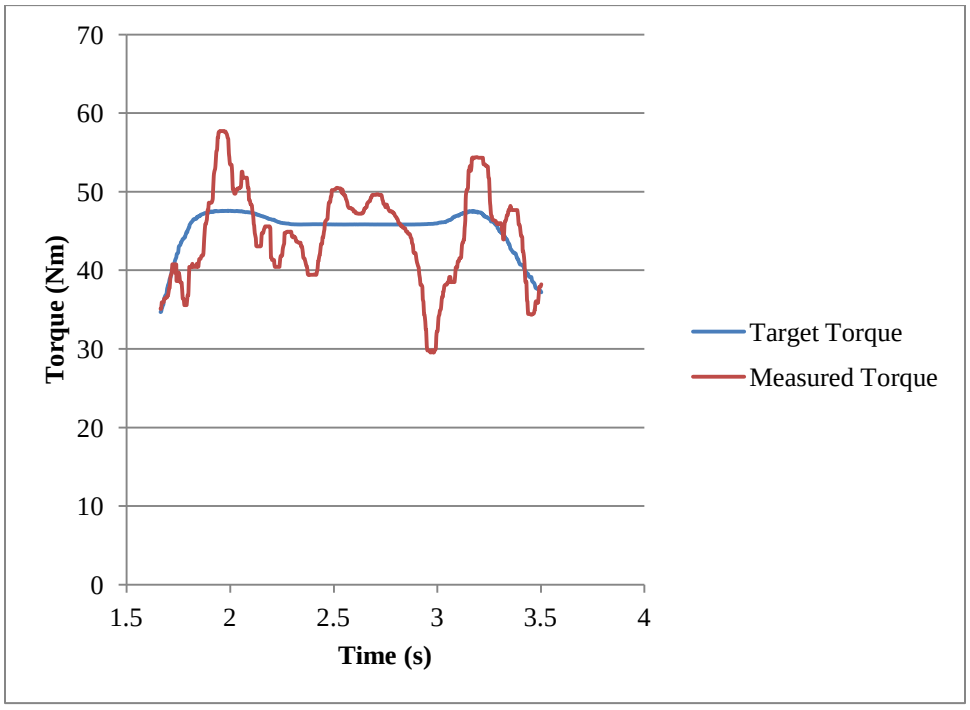

Figure 4.1: Example of Overshooting

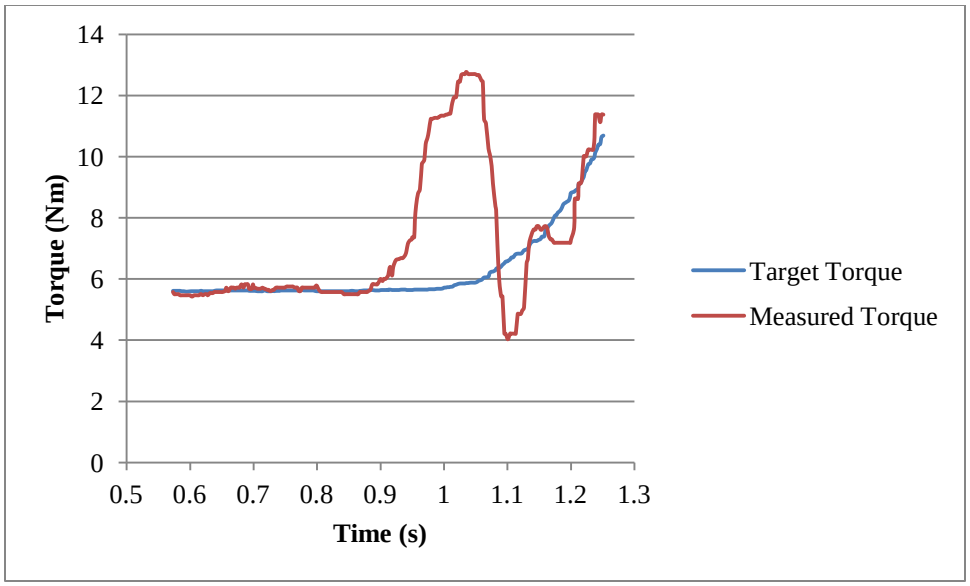

Figure 4.2: Peak in Measured Torque at Start of Torso Flexion

These peaks are caused by the torso pushing on the load cell as it starts to move and are only a fraction of a second or about 0.2 seconds in duration. The support then responds to this movement. The peaks may be reduced by making the system more responsive. However, care must be taken so it does not become so responsive it overshoots the target. If this were to happen, it would introduce additional instability.

Another observation post-hoc is the discrepancy shown in Figure 4.3, which occurs between the end of a lower and beginning of a lift. Since the gap starts at an inflection point, it could be the result of the change in direction of the torso. As the torso is travelling downward, it is putting a force on the load cell. When it reaches the inflection point, it is no longer travelling downward so this force disappears. The support recognizes this and increases the amount of torque until the load cell measures a change. It takes some time for this to occur because the support motor was not producing much torque and overshoots as a result (indicated by the peak in the figure below). Also the torso is starting a lift.

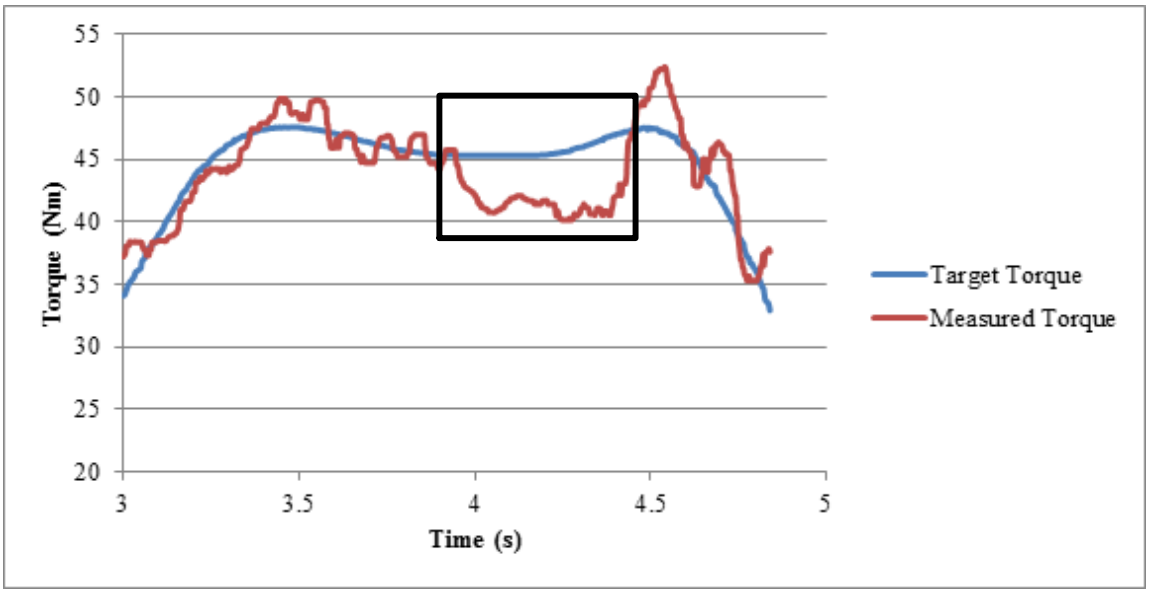

Figure 4.3: Descrepancy During Maximum Torso Flexion

4.3 Torso Motor Torque

Figure 3.8 through Figure 3.10 show a reduction in the amount of positive torque needed to move the torso through the trajectory. An increase in negative was observed also. Reasons for this are discussed in the next section.

4.3.1 Negative Torque

Negative torque was needed more frequently for higher levels of assist (see Figure 3.8, Figure 3.9, and Figure 3.10). At higher levels of assist, less and less of the torso's weight was available for the torso to use to achieve the desired response. For example, at 100% assist, ideally all of the torso's weight is supported. Since it was fully supported, the torso motor could not simply reduce the amount of torque it provided, allowing the load cell to measure the increased load. The torso motor needed to apply negative torque for the load cell to measure the increase.

The torso motor had to apply a large negative torque during the start of some lowers, even with no assist. The greatest amount of negative torque was applied at the beginning of the multiple lifts with pauses trajectory. It was suspected that gravity alone was insufficient to accelerate the torso. To determine if this was the case, the vertical acceleration of the trajectory was compared to the vertical acceleration calculated for a freefalling mass about a fixed point. The vertical acceleration of the C7 marker in the multiple lifts with pauses trajectory was compared to the vertical acceleration of the torso if it were treated like a freefalling inverted pendulum. The acceleration of the C7 marker was found using Vicon Motus. The acceleration of the inverted pendulum was found using the free body diagram in Figure 4.4.

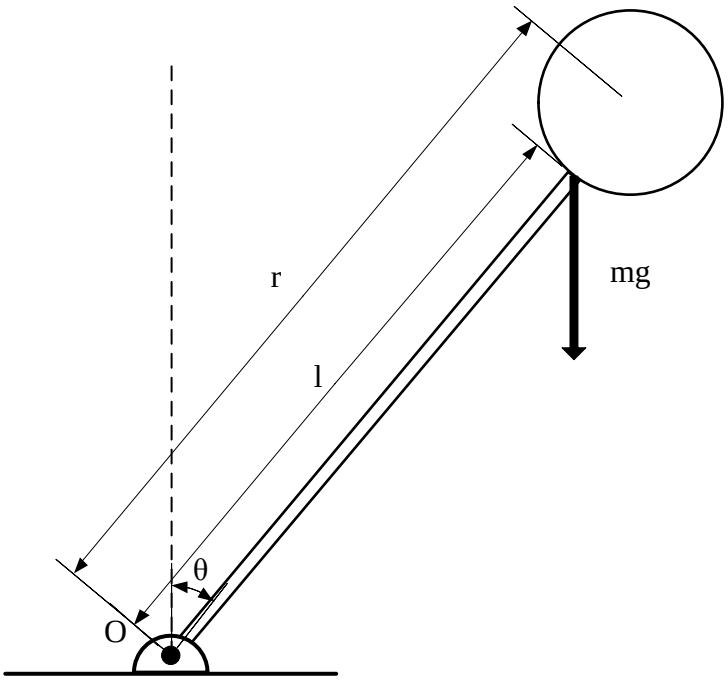

Figure 4.4: Freebody Diagram of Inverted Pendulum

Using this diagram the moments were summed about point O (Equation 4.1), where M_O are the moments acting on point O, I_O is moment of inertia of the body rotating about point O, and $\ddot{\theta}$ is the angular acceleration of the pendulum.

$$\sum M_O = I_O \ddot{\theta} \qquad \text{Equation 4.1}$$

Summing the moments gives the following equation,

$$-mgl \sin\theta = I_O \ddot{\theta} \qquad \text{Equation 4.2}$$

where m is the total mass of the torso, g is the acceleration due to gravity, and l is the distance from point O to the center of mass. The torso's mass and its location were found using Solidworks. Solving for the angular acceleration gives Equation 4.3.

$$\ddot{\theta} = \frac{-mgl \sin\theta}{I_O} \qquad \text{Equation 4.3}$$

The angular acceleration is related to tangential acceleration by the following relationship shown in Equation 4.4.

$$a_t = r\ddot{\theta} = \frac{-mglr \sin\theta}{I_O} \qquad \text{Equation 4.4}$$

The acceleration in the normal direction also affects vertical acceleration. The normal acceleration can be found by starting with Equation 4.5 and substituting Equation 4.3 in for $\ddot{\theta}$.

$$\dot{\theta}\, d\dot{\theta} = \ddot{\theta}\, d\theta \qquad \text{Equation 4.5}$$

$$\int_0^{\dot{\theta}} \dot{\theta}\, d\dot{\theta} = \frac{-mglr}{I_O} \int_0^{\theta} \sin\theta\, d\theta \qquad \text{Equation 4.6}$$

Integrating on both sides results in Equation 4.7.

$$\dot{\theta}^2 = \frac{-mglr}{I_O}(\cos\theta - 1) \qquad \text{Equation 4.7}$$

The normal acceleration is related to angular velocity by Equation 4.8

$$a_n = r\dot{\theta}^2 = \frac{-mglr^2}{I_O}(\cos\theta - 1) \qquad \text{Equation 4.8}$$

and the vertical acceleration was determined using Equation 4.9.

$$a_v = a_n \cos\theta + a_t \sin\theta \qquad \text{Equation 4.9}$$

The maximum vertical acceleration of the C7 marker was about -4 m/s^2 and occurred at approximately 10 degrees from vertical. The vertical acceleration of the torso was estimated to be only -0.37 m/s^2 at 10 degrees (see Figure 4.5) if it was freefalling.

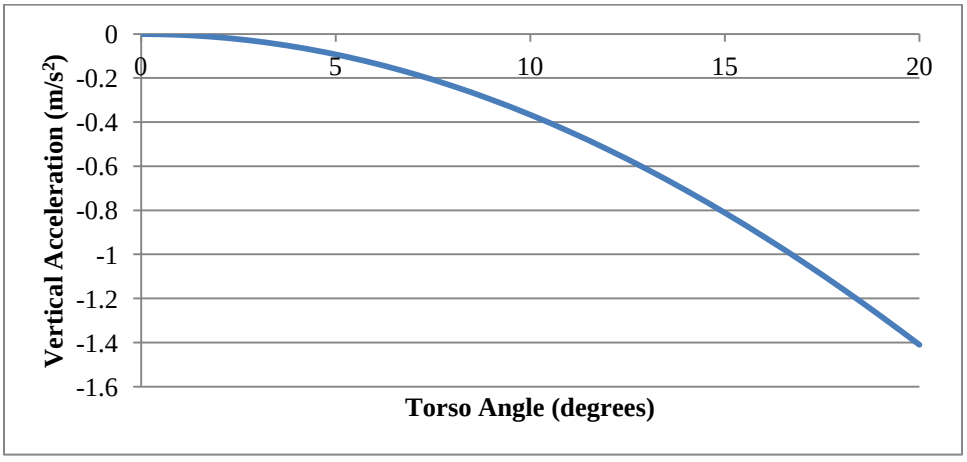

Figure 4.5: Vertical Acceleration of Freefalling Inverted Pendulum

It can be concluded that gravity was not sufficient to accelerate the torso so it would follow the trajectory and additional torque was needed by the torso motor to match the trajectory.

The percent of assist was proportional to the amount of negative torso the torso motor had to produce. In other words, the greater the level of assist, the more negative torque the torso motor had to generate. This is illustrated in Figure 3.8, Figure 3.9, and Figure 3.10. This is likely because the support only assists in one direction. Negative torque is needed to accelerate the torso because gravity is insufficient to achieve this motion alone. The support applied a force which adds torque in the opposite direction, requiring more from the torso motor. The support control was designed to apply a certain amount of force to the torso to assist it throughout torso movement. Since the goal of this device is to reduce erector spinae muscle activity, perhaps the support control should be redesigned to only maintain contact during torso flexion and apply a minimal amount of force to the torso or even help accelerate the torso downward.

4.4 Limitations and Differences From Real Device

There are limitations of the torso apparatus used to simulate torso motion and the support. The torso was limited to one degree of freedom and the legs of the apparatus were fixed vertically. Since the legs were fixed in this position, the torsion spring angle was the same as the support angle. The torsion spring angle will be the hip angle on an actual device and will need the appropriate sensors to measure this angle. The control system will need to be modified to use these additional sensors. The torso angle will need to be approximated by an inclinometer or similar sensor type. This would provide a

measurement which does not depend on the position of another part of the body, which may be desirable. Because of symmetry, the torso and support constructed for this research only provided support one on side. An actual device would duplicate sensors, motors, and springs for each side. As a result, the control system will need to be able to handle the additional inputs and outputs.

4.5 Other Improvements

Based on the results of the analysis, changes will probably be needed to improve the support system. First, using different PID gains for each assist level could improve the response of the support. Also, using different PID gains depending on angular acceleration/velocity and position may further improve the support. User inputs could also be used to determine the responsiveness and feel of the assist to make it more comfortable. The support control could also include the ability to adapt to the wearer's motion and patterns, which may provide a more comfortable response. Also, the system may benefit from antiwindup techniques, which may reduce overshoot.

Safety measures need to be integrated to reduce or eliminate hazards associated with using a wearable device. These may include a feature to turn off the device if certain angles (realistic or not) are measured. Also, steps should be taken to limit the rate torque is increase and decreased. If there is a sudden large force detected, the device should respond appropriately. Certain ranges of acceptable measurements and calculation results may be necessary. The safety of the user is paramount.

5. CONCLUSION

The purpose of this project was to develop a control for a lift assist device, which could support the upper body. To test the control system, the torso's trajectory, load cell measurements, and torque produced by the torso motor were analyzed. There was a statistical difference comparing the torso's trajectory with no assist to the trajectory with each assist level. Although there was a statistical difference, there may not be a practical difference. Graphically the trajectories appear similar because of the overlap. The torso's trajectory may always be affected to some degree, when the support is used, because force is being applied to the upper body. No statistical difference was detected between the measured torque from the load cell and the desired value. There were some points during the torso's trajectory where too much force was applied on the torso. These can be reduced by increasing the responsiveness at the start of torso flexion and increasing damping at the end of a lower. For the most part the correct amount of support was measured throughout the trajectory. The torso motor torque, which analogous to muscle force, decreased during lifting (positive torque) but increased during a lower (negative torque). This implies that erector spinae muscle force was reduced but rectus abdominus muscle force increased. The increased torque in the negative direction was likely caused by the support applied force to the torso. The current control system was designed to apply force during torso flexion. Increased negative torque values may be a tradeoff of the current design. After an active device is constructed future research could

include the effects of increased rectus abdominus activity and if the support control should be modified during torso flexion.

A wearable active lift assist device could have a variety of applications. Since the device is capable of providing different levels of assist it could be very useful in rehabilitation after low back surgery or injury. It could be used in hospitals for inpatient or outpatient rehabilitation or even home use. Physical therapy clinics may also benefit. At the beginning of a rehabilitation program it could support much, if not all, of the upper body during lifting or torso movement. Over the course of the rehabilitation program, the assist level could be lowered allowing the muscles in the low back to strengthen by slowly allowing them to support the upper body. Each assist level and its duration could be a part of a predefined program or timetable. This could eliminate the need for user input after the device is set up and reduce the chance of the wrong assist level being used. It may also be desirable to not allow the user to change the assist level. This timetable may be integrated into the lift assist device's software so assist level is adjusted automatically. A device of this type would not necessarily be limited to low back surgery or pain. It could be used as a part of rehabilitation for other injuries or surgeries. Future work should include an investigation of other injuries or surgeries this could be used to treat.

It could also be used in the occupational setting by those suffering from low back pain, since BCF is attributed to pain in that area. Using it while performing frequent lifting and other manual material handling tasks could prevent low pain injuries and may help relieve already occurring low back pain. Surgeons, mechanics, and others whose job requires standing with the torso flexed for extended periods of time would also benefit

from this device, as their upper bodies could be entirely supported. The advantage a wearable device has over others attached to a wall or floor is mobility. The wearer is not limited by a track or its limited range of motion. Also, a wearable device does not require any modification of working environments for installation.

The next step is to create a prototype to explore the benefits of its use and its viability in rehabilitation and physical therapy. Research should be performed to determine the effectiveness of the device by measuring erector spinae and rectus abdominus muscle activity using electromyography (EMG). Its use to relieve low back pain and prevent injuries may also be of interest, as well as other uses.

REFERENCES

Bureau of Labor Statistics. (2009). Nonfatal cases involving days away from work: Selected characteristics (2003). Retrieved March 24, 2011, from http://data.bls.gov/cgi-bin/dsrv?ch.

Deyo, R. A. (2007). Back surgery--who needs it?. *N Engl J Med, 356* (22), 2239-2243.

Drillis, R., & Contini, R. (1966). Body Segment Parameters. *Technical Report 1166-03*. New York, NY: New York University School of Engineering Science.

Gray, H. (1918). *Anatomy of the Human Body.* (18th ed.). Philadelphia, PA: Lea & Febiger.

Jenkins, D. B. (1991). *Hollinshead's Functional Anatomy of the Limbs and Back* (Sixth ed.). Philadelphia, PA: W.B Saunders Company.

Katz, J. N. (2006). Lumbar disc disorders and low-back pain: socioeconomic factors and consequences. *J Bone Joint Surg Am, 88 Suppl 2*, 21-24.

Kumar, S. (2008). *Biomechanics in Ergonomics* (Second ed.). Boca Raton, FL: CRC Press.

LeBlanc, K. E., & LeBlanc, L. L. (2010). Musculoskeletal disorders. *Prim Care, 37* (2), 389-406.

Marras, W. S., Ph. D. (2008). *The Working Back: A Systems View*. Hoboken, NJ: John Wiley & Sons, Inc.

McGregor, A. H., Burton, A. K., Sell, P., & Waddell, G. (2007). The development of an evidence-based patient booklet for patients undergoing lumbar discectomy and un-instrumented decompression. *Eur Spine J, 16* (3), 339-346.

National Institute for Occupational Safety and Health. (2004). Worker Health Chartbook, 2004. (2004–146). Retrieved May 19, 2011 from http://www.cdc.gov/niosh/docs/2004-146/pdfs/2004-146.pdf.

National Instruments. PID theory explained. (Mar 29, 2011). Retrieved December 27, 2011, from http://zone.ni.com/devzone/cda/tut/p/id/3782.

Pai, S., & Sundaram, L. J. (2004). Low back pain: an economic assessment in the United States. *Orthop Clin North Am, 35* (1), 1-5.

Pope, M. H. (1989). Risk indicators in low back pain. *Ann Med, 21* (5), 387-392.

Snodgrass, J. (2011). Effective occupational therapy interventions in the rehabilitation of individuals with work-related low back injuries and illnesses: a systematic review. *Am J Occup Ther, 65* (1), 37-43.

Waters, T. R., Putz-Anderson, V., Garg, A., & Fine, L. J. (1993). Revised NIOSH equation for the design and evaluation of manual lifting tasks. *Ergonomics, 36* (7), 749-776.